JCTC Journal of Chemical Theory and Computation

pubs.acs.org/JCTC Article

Solving the Scaled Schrödinger Equation with SAC−CI and Electrostatic Force Formalism. Ground, Excited, and Ionized States of the Benzene Molecule

Hiroshi Nakatsuji*

Cite This: https://doi.org/10.1021/acs.jctc.5c02112 Read Online

ACCESS | Metrics & More | Article Recommendations | Supporting Information

ABSTRACT: An exact theory for solving the scaled Schrödinger equation (SSE) has been extended to molecular ground, excited, and ionized states that satisfy the Hellmann−Feynman electrostatic force (ESF) theorem, a necessary condition for the exact wave function. This is realized by applying the free complete-element (FC) or SSE theory to the symmetry-adapted-cluster (SAC) configuration-interaction (CI) wave functions that are designed to satisfy the ESF theorem. The resultant theory, called the FC or SSE(SAC−CI, ESF) theory, is not only highly accurate but also predictive, using both energetic and force theoretic concepts. Here, this theory is applied to a benzene molecule, a 42-electron molecule, the largest system yet treated by our exact theory. Notably, the theory resolved complex features of higher singlet and triplet excited states of a benzene molecule, which had previously eluded conventional methods.

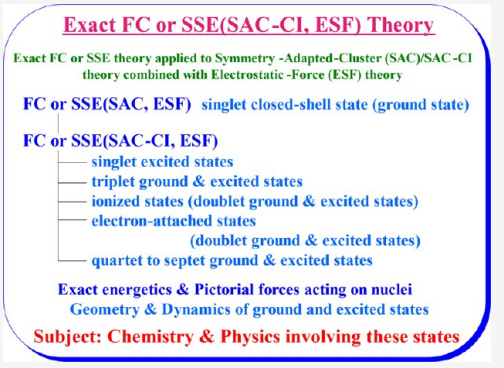

1. INTRODUCTION

In natural science, what is often referred to as "the God equation"[1] is important, whose predictions must be accurate and intuitively sharp. In classical mechanics, Newton's equation serves this role, as it is conceptually simple and computationally solvable. In quantum mechanics, the Schrödinger equation (SE)

$$(H - E)\psi = 0 \tag{1}$$

holds this status, where H is the Hamiltonian given in the Born−Oppenheimer approximation by

$$H = \sum_i -\frac{1}{2}\Delta_i - \sum_i \sum_A Z_A/r_{Ai} + \sum_{i>j} 1/r_{ij} + \sum_{A>B} Z_A Z_B/r_{AB} \tag{2}$$

where r is a distance, and the suffices i, j run for electrons and A, B for nuclei. E and ψ are the energy and wave function, respectively, of the system. In eq 2, the first term represents the kinetic energy operator, with Δ_i being the Laplacian $\Delta_i = \partial^2/\partial x_i^2 + \partial^2/\partial y_i^2 + \partial^2/\partial z_i^2$. The second-to-last terms are Coulomb attraction and repulsion terms between electrons and nuclei that diverge at the point where particles collide with each other. The SE is believed to be a governing principle of atoms and molecules when relativistic effects are small. It is very important to find a general method of solving the SE for understanding and predicting phenomena occurring in chemical science. However, as Dirac famously remarked[2] many years ago, direct analytical solutions of this equation had been impossible for realistic systems, except for a very simple system like the hydrogen atom. Then, exact predictions in chemistry and physics based on exact solutions of this equation have long been impossible. Indeed, it is truly important to find a method of obtaining exact solutions of the SE.

As such method, we may use the variational principle

$$\langle \delta\tilde{\psi}|H - E|\tilde{\psi}\rangle = 0 \tag{3}$$

to solve the SE, where $\tilde{\psi}$ is a trial approximate wave function. Here, the problem is what form do we assume for the function $\tilde{\psi}$? When we assume a single determinant for $\tilde{\psi}$, we get Hartree−Fock wave functions for $\tilde{\psi}$, but it is far from exact. The same is true: when we assume an exponential function for $\tilde{\psi}$, we get a coupled cluster wave function, but it is not exact, again. A good idea might be to assume $\tilde{\psi}$ as

$$\tilde{\psi} = \tilde{\psi}(H) \tag{4}$$

because the exact wave function must be a functional of its Hamiltonian as the SE suggests. However, when we put eq 4 into eq 3, we get the variational formula diverging to infinity

$$\langle \delta\tilde{\psi}|H - E|\tilde{\psi}\rangle = \pm\infty \tag{5}$$

Received: December 18, 2025
Revised: February 26, 2026
Accepted: February 26, 2026

instead of zero, because there are three $1/r$ terms in the bra, Hamiltonian and ket of eq 3 and therefore, there is no way to make this variational formula becoming equal to zero. This situation continued until say 2000.

On 2000, this author initiated the study on the structure of the exact wave function,[3] to obtain basic insights necessary for finding a general method of exactly solving the SE. He studied orthodox theories, exponential theories, inverse theories, etc., and in 2004, he published the scaled Schrödinger equation (SSE)[4] written as

$$g(H - E)\psi = 0 \tag{6}$$

where g is a function of r, $g(r)$, referred to as the scaling function.[4,5] It was defined as always positive (or equivalently always negative). Then, it is clear that the SSE always has the same set of solutions, as the original SE. Therefore, physically, the SSE is equivalent to the SE. However, with the SSE, the variational formula, $\langle \delta\tilde{\psi}|g(H - E)|\tilde{\psi}\rangle$, does not diverge and can be made equal to zero, leading to correct exact solutions as

$$\langle \delta\tilde{\psi}|g(H - E)|\tilde{\psi}\rangle = 0 \tag{7}$$

differently from eq 5 for the SE. Then, we can utilize the variational formula even for exactly solving the SSE.

Thereafter, a general theory of solving the SSE was formulated[6−15] and referred to as free complete-element (FC) theory. (The old naming, free "complement" theory was misleading and is withdrawn hereafter.) The physics of the g function was studied.[14,15] As r approaches zero, g must become proportional to r, and as r becomes infinity, g must converge to unity. Several mathematical functions were presented,[14] and the one used in this paper has the following form

$$g = 1 - \exp(-\gamma r) \tag{8}$$

The SSE is solved straightforwardly as[4]

$$\psi = \exp[Cg(H - E)]\psi_0 \tag{9}$$

using only one single variable C and an approximate initial function ψ_0. This formula was called the simplest ECC (extended coupled cluster) formula. Alternatively, the SSE is solved in a recursion formula as[4]

$$\psi_n = [1 + C_n g(H - E_{n-1})]\psi_{n-1} \tag{10}$$

where ψ_n is the n-th order approximation of the exact wave function. This equation, called the simplest iterative configuration interaction (SICI) equation,[4] is not efficient actually because it includes diverging functions. So, we expand the right-hand side of eq 10 up to the sum of elemental analytical functions and then keep only the nondiverging functions $\{\phi_I^{(n)}\}$ and obtain[4]

$$\psi_n = \sum_I c_I^{(n)} \phi_I^{(n)} \tag{11}$$

We continue this formulation by increasing n until the convergence to the exact wave function. Then, we obtain a set of functions $\{\phi_I^{(n)}\}$ that is a complete set of functions that spans the exact wave function as given by eq 11. Thus, we have made up free complete-element functions to construct the exact wave function. So, we call this theory free complete-element (FC) theory, replacing the old naming, free "complement" theory that was misleading. Further, the above theory is just equivalent to solving the SSE given by eq 6, and so this theory may also be referred to simply as SSE theory, as given in the abstract and in the TOC graphic.

The theory explained above has been applied to many atoms and molecules and has produced essentially exact solutions.[4−15] For example, by applying this theory to a helium atom, we could obtain its ground state energy correct to over 40 digits.[8,9] More recently, we applied this theory to the Li_2 molecule[13] and obtained its nine valence-state potential energy curves, which completely reproduced the experimentally observed potential curves in absolute accuracy.[13] The equilibrium distances and the vibrational properties of Li_2 all agreed well in high accuracy with the available experimental data. These results show that the present theory that solves the SE or SSE has a potentiality of reproducing chemistry as it is, as long as relativistic effects are small. However, so far, applied systems have been rather small because we mainly used VB (valence bond) type formalisms.

2. PROPOSAL OF A NEW THEORY

We propose here a new exact theory in an MO (molecular orbital) formalism and aim to describe various electronic states, namely, ground, excited, ionized, and anion states of a molecule, at the same time. This is achieved by applying the FC or SSE theory to the SAC (symmetry-adapted cluster)[16]/SAC−CI formalism.[17] So, before describing the new theory, we briefly explain the SAC/SAC−CI formalism.

The SAC theory[16] is a kind of coupled-cluster theory[21−25] in a symmetry-adapted form which is necessary for nonlinear expansions like coupled-cluster theories. Exponential generation formalism is efficient and suitable for describing correlation effects to higher orders, as studied generally by this author in 1985.[18] The SAC−CI theory[17] describes singlet, triplet, and even higher-spin multiplet excited states and ionized, anion states of the same molecule. This theory utilizes the best-optimized functional space produced by SAC formalisms and therefore is efficient and balanced well with the SAC wave function.[17−20] The SAC/SAC−CI approach has been proven effective and accurate in many interesting phenomena,[19,20] which include highly accurate studies of excited and ionized states of benzene molecules,[26] collision-induced spectroscopy,[27] fine spectroscopy,[28] electron transfers in the photosynthetic reaction center of a purple bacteria, *Rhodopseudomonas viridis*,[29,30] photoemission of firefly,[31] et cetra. The SAC/SAC−CI code is therefore very useful for various studies involving ground, excited, ionized, and electron-attached states of molecules. It was implemented in the Gaussian software package[32] and has been used worldwide. With this formalism, it is possible to study various electronic states of general molecules at a time. We note that the so-called "EOM-CC"[33,34] is just the same[35] as SAC−CI, which was published about a decade earlier[16,17,24,25] than "EOM-CC". Priority and originality are something most important in science and the scientific community.

Thus, we understand the importance of the present subject, namely, upgrading the SAC/SAC−CI formalism to the exact level by applying the FC or SSE theory. Further, the present theory must satisfy the Hellmann−Feynman electrostatic force (ESF) theorem[36,37] because this theorem is a necessary condition for the wave function to be exact. There are several methods for satisfying the ESF theorem. One is to float basis functions variationally from nuclear centers, the so-called floating method,[38] but this method is not so efficient from energetic points of view. A more popular and efficient method, which we adopt here, is to add derivative bases to already

https://doi.org/10.1021/acs.jctc.5c02112
J. Chem. Theory Comput. XXXX, XXX, XXX−XXX

existing bases. This method is efficient for satisfying the ESF theorem and for improving, at the same time, the quality of the wave function.[39] Further, importantly, one can utilize simple and intuitive ESF concepts for molecular structures and chemical reactions developed by this author in 1973−4.[40−43] Further, dynamic behaviors of electron densities of a molecule undergoing changes in nuclear configurations, like in molecular vibrations and chemical reactions, could be viewed in a general fashion as electron-cloud incomplete following and preceding courses of nuclear rearrangement processes.[42,43] The force concept in chemistry summarized in a book[44] by Deb, Bader,[46] and myself[45] is useful even in exact theories developed in my laboratory. When the ESF theorem is satisfied, time-consuming energy-gradient calculations become unnecessary.

Thus, we refer to the present exact theory as FC or SSE(SAC−CI, ESF) theory. We apply this exact theory to the set of SAC−CI wave functions for ground, excited, and ionized states, which are expanded with basis functions that incorporate their derivative bases to satisfy the ESF theorem and obtain potentially exact wave functions that are correct in both energy and force formalisms. There, the additional force concepts are very useful because the basic electrostatic force view is described only with electron clouds surrounding nuclei. Molecular geometries and chemical reactions are studied using electrostatic forces acting on nuclei due to electron clouds nearby nuclei along nuclear rearrangement processes.[40−43]

Actual procedures to produce such exact wave functions are as follows. First, we choose a simple initial set of basis functions and calculate initial SAC/SAC−CI wave functions for ground, excited, and ionized states. Next, to make the ESF theorem satisfied, we add derivative basis functions and apply the SAC/SAC−CI theory. This is the initial set of functions for the present theory. Then, we apply the FC theory and continue the whole process until the convergence by increasing the order n of the FC theory. The resulting framework, FC or SSE(SAC−CI, ESF) theory, synergistically combines:

- the rigor of the FC or SSE theory,
- the practical wide applicability of the SAC/SAC−CI theory, and
- the intuitive clarity of the ESF theory.

Because the SAC/SAC−CI theory has already been applied to large molecular systems like the photosynthetic reaction center,[29] the present FC or SSE(SAC−CI, ESF) theory is expected to expand the limit of the exact theory in practical areas of chemistry. Further, because the present theory satisfies the ESF theorem, we can utilize its simple concepts to intuitively understand and to predict the underlying chemistry. The ESF concept[40−43] is unique and correct even to the exact limit. Thus, now, a computationally exact yet broadly applicable and further intuitively predictive theory has been established.

Performing computational parts of this theory with a quantum computer is fascinating. Then, much scaling up of sizes of applied systems and substantial speed-up in computations are expected. Below, the newly developed FC or SSE(SAC−CI, ESF) theory is applied to the benzene molecule, C_6H_6. This is a key compound of chemistry, as historically studied by Kekule.

3. INCREASING ACCURACY WITH THE FC OR SSE(SAC−CI, ESF) THEORY

In 1987, the present author studied benzene molecule[26] with his own SAC−CI code[16,17,32] and clarified the natures of valence and Rydberg excited states of this molecule. Though basic natures of the ground and lower excited states were clarified, some difficulties remained particularly in clarifying the nature of the 1^1E_{2g} excited state at around 7.8 eV.[26]

In the present study, we study this molecule with substantially higher accuracies of the FC SSE theory than any earlier studies have. The geometry of the benzene molecule was fixed at the experimental ground-state one,[47] R_{C-C} = 1.397 Å and R_{C-H} = 1.084 Å. All excited and ionized states were calculated at this geometry, i.e., vertical states. We initiated calculations using minimal Slater-type orbitals (STO's) with exponents from Slater's rule.[48] With this rule, the exponents of the 2s and 2p orbitals are the same, and so the derivative bases necessary for the Hellmann−Feynman theorem are only d STO's with the same exponents. They form the so-called shell structure, which is very favorable for the satisfaction of the Hellmann−Feynman theorem. This was confirmed by the test calculations for the CO molecule using a similar set of basis functions by calculating both energy gradients and Hellmann−Feynman forces, though such calculations are huge for the benzene molecule. In the present calculations, we consider only g_{iA}-type scaling functions that are integrable, and the calculations were performed using a Gaussian program using the STO-20G expansion method. However, we did not include g_{ij}-type scaling functions, because they are not integrable. The SAC/SAC−CI formalism incorporates correlation effects partially. Sampling-type methodology is not welcome for routine calculations. From this last limitation, the present calculation does not reach an absolutely exact level of accuracy. However, remarkably, even from such crude initial functions, the present new theory yields highly accurate results as shown below.

It would be interesting to visualize the systematic approach to the exactness, increasing the order of the FC theory. We wanted to understand the mechanism step by step. For this purpose, the calculations were performed across six levels below

Level 1; single minimal STOs

Level 2; + x, y, z derivative bases

Level 3; + FC(n = 1)

Level 4; + FC(n = 2)

Level 5; + Rydberg 3s, 3p, 3d bases on each carbonatom

Level 6; + FC(n = 3) + Rydberg 4s, 4p, 4d bases on the molecular center

where +means added bases and/or operation. We started from the simplest possible initial choice, i.e., single minimal STO's at Level 1, and then their derivative bases are added at Level 2. From Level 3, we applied the FC theory to make the system approach toward exactness. After order 2 at Level 5, we added third-row Rydberg bases[49] on carbon as s, p, d, primitive minimal Slater bases with the exponent of 0.48, altogether. At Level 6, we raised the FC order to three and added fourth-row Rydberg bases, which are the s, p, an d, primitive minimal Slater basis, with the exponent 0.25 on the center of molecule.[49] Because the simple orbital model is enough for Rydberg states, we did not add any derivative bases and did not apply FC theory. As far as the inner valence states are accurately described, a simple orbital model would be enough for Rydberg states because they are simple, one electron-like states surrounding the positively charged inner molecular region. Up to order 2 of the

https://doi.org/10.1021/acs.jctc.5c02112
J. Chem. Theory Comput. XXXX, XXX, XXX−XXX

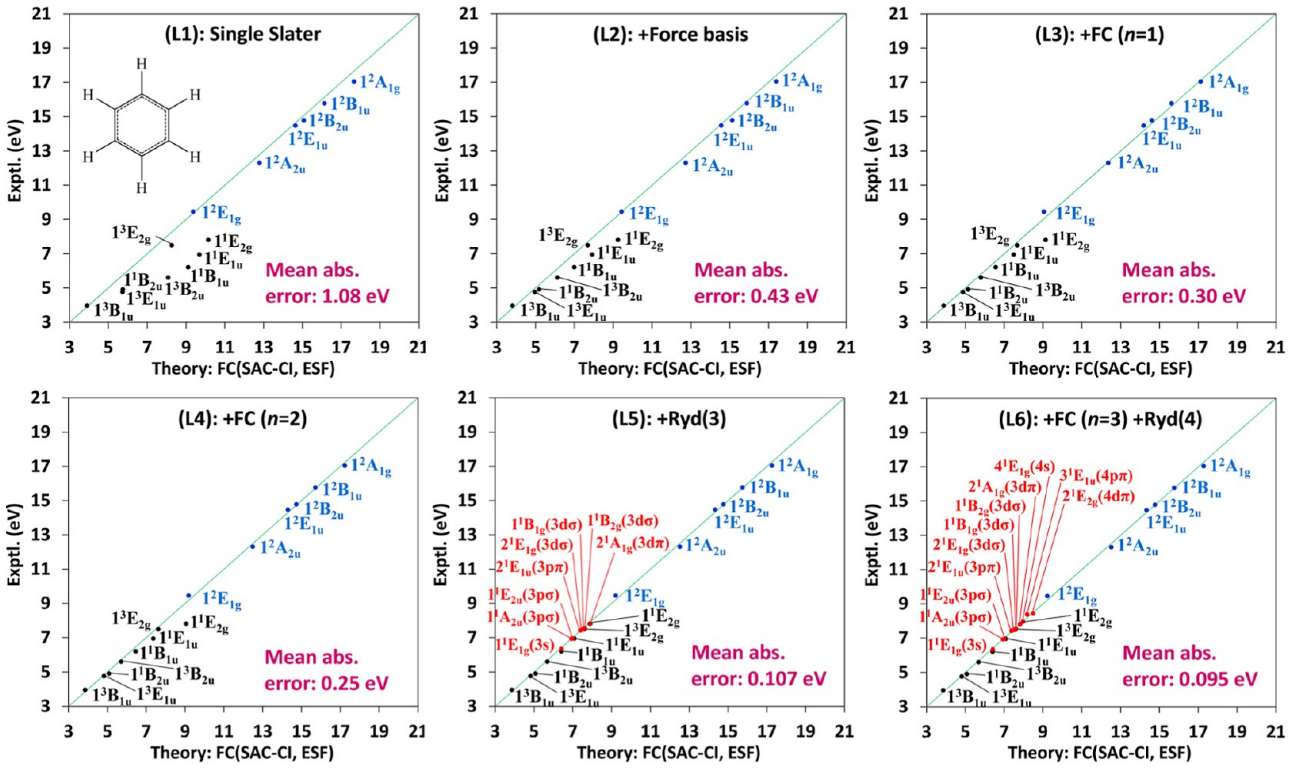

Figure 1. Comparisons of six different levels of the present theory and experiments for singlet and triplet valence (black) and Rydberg (red) excitations and ionizations (blue) of the benzene molecule. Each different level of the theory is explained in the text. The mean absolute error at each level is shown in pink in eV units.

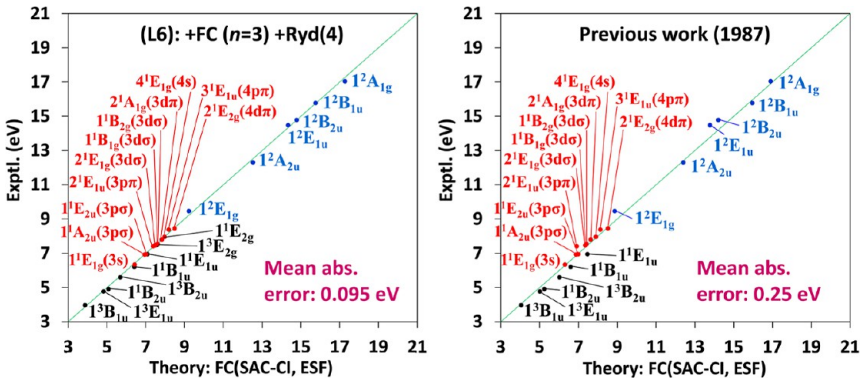

Figure 2. Excitation and ionization energies of the L6 level of the present theory compared to that of previous SAC−CI calculations in 1987.

FC theory, the computer time was 4 days 2 h 32 min, and up to order 3 with Rydberg bases, it was 7 days 8 h 26 min with computers at the IMS computer center, Okazaki.

Figure 1 shows a compact summary of the calculated results of vertical excitation energies and ionization energies from Level 1 (L1) to Level 6 (L6). They are compared against experiments using the 45-degree line. At L1, the basis set is minimal, the simplest-possible basis set, but even so, SAC−CI results are reasonable with a mean absolute error (MAE) of 1.08 eV. Large errors are due to discrepancies in some singlet and triplet valence excited states. Notably, ionized states (shown in blue) align closely on the 45° line, and this is so even across all six levels of the theory. Maybe ionized states could be described well with the SAC−CI theory even with a small basis set. Then, by adding derivative bases at the L2 level, calculated results were improved largely, and the MAE value reduced to less than half, 0.43 eV. Then, we applied the FC theory to order one, and the MAE reduced to 0.30 eV (L3) and 0.25 eV at $n = 2$ (L4). However, the $^1E_{2g}$ state still deviates notably from the 45-degree line. However, upon adding third-period Rydberg bases at the L5 level, many higher singlet excited states, including the $^1E_{2g}$ state, were dramatically improved, reducing the MAE to 0.107 eV. This suggests substantial valence−Rydberg mixings in these states. Finally (L6), with FC $n = 3$ and fourth-period Rydberg functions added, the MAE decreased to 0.095 eV, indicating the convergence. Here, all states are well along the 45-degree line.

Several important points are summarized: (1) singlet states are rather complex, in comparison with triplet and ionized states. A highly accurate theory like the present one is necessary to describe the complex natures of higher singlet excited states. (2) Triplet states converge more rapidly than singlet states. Ionized states are consistently accurate from the beginning. (3) Coming back to level L1, we explain why we chose such crude bases initially. One is to show that the FC theory can give exact results

https://doi.org/10.1021/acs.jctc.5c02112
J. Chem. Theory Comput. XXXX, XXX, XXX−XXX

Table 1. Excitation Energies (ExtE) and Ionization Energies (IE) Compared to the Experimental Data for Low-Lying Singlet and Triplet Valence and Rydberg Excited States and Ionized States of Benzene, Calculated by the Present Theory at Level 6

No	State	Pair	Orbital picture	Excitation energy (ExtE)(eV)	Exptl. ExtE (eV)	Δ(ExtE)[a]	Oscillator strength	Second moment (au)
1	X^1A_{1g}			(−231.985 030)[b]				78.4
2	1^1B_{2u}		$\pi_2 \rightarrow \pi_3^*$	5.078	4.90[c]	0.18	0	79.9
3	1^1B_{1u}		$\pi_2 \rightarrow \pi_3^*$	6.412	6.20[c]	0.21	0	82.5
4	1^1E_{1g}		$\pi_2 \rightarrow 3s$	6.421	6.33[d]	0.09	0	128.8
5	1^1A_{2u}		$\pi_2 \rightarrow 3p\sigma$	6.945	6.93[e]	0.01	0.087	151.6
6	1^1E_{2u}		$\pi_2 \rightarrow 3p\sigma$	7.019	6.95[e]	0.07	0	154.5
7	1^1E_{1u}		$\pi_2 \rightarrow 3p\pi$, $\pi_2 \rightarrow \pi_3^*$	7.089	6.95[c]	0.14	0.468	126.9
8	1^1A_{1u}		$\pi_2 \rightarrow 3p\sigma$	7.112			0	159.2
9	2^1E_{1u}		$\pi_2 \rightarrow \pi_3^*$, $\pi_2 \rightarrow 3p\pi$	7.386	7.41[f], 7.19[g]	−0.02, 0.20	0.514	116.5
10	2^1E_{1g}		$\pi_2 \rightarrow 3d\sigma$	7.496	(7.46)[h]	(0.04)	0	146.4
11	1^1B_{1g}		$\pi_2 \rightarrow 3d\sigma$	7.603	(7.54)[g]	(0.06)	0	182.3
12	1^1B_{2g}		$\pi_2 \rightarrow 3d\sigma$	7.613	(7.54)[g]	(0.07)	0	185.4
13	3^1E_{1g}		$\pi_2 \rightarrow 3d\sigma$	7.622			0	183.3
14	1^1E_{2g}		$\pi_2 \rightarrow 3d\pi$, $\pi_1 \rightarrow \pi_3^*$[i]	7.822	7.80[j], 7.81[g]	0.02, 0.01	0	228.3
15	2^1A_{1g}		$\pi_2 \rightarrow 3d\pi$	7.836	7.80[g]	0.04	0	238.5
16	1^1A_{2g}		$\pi_2 \rightarrow 3d\pi$	7.862			0	240.8
17	4^1E_{1g}	4	$\pi_2 \rightarrow 4s$	7.971	7.95[g]	0.02	0	423.4
18	2^1A_{2u}	5	$\pi_2 \rightarrow 4p\sigma$	8.141			0.018	470.5
19	2^1E_{2u}	6	$\pi_2 \rightarrow 4p\sigma$	8.161			0	480.4
20	2^1A_{1u}	8	$\pi_2 \rightarrow 4p\sigma$	8.186			0	489.3
21	3^1E_{1u}		$\pi_2 \rightarrow 4p\pi$	8.193	8.37[f]	−0.18	0.000	465.8
22	3^1A_{2u}		$\sigma_8 \rightarrow \pi_3^*$	8.208			0.006	87.3
23	3^1A_{1u}		$\sigma_8 \rightarrow \pi_3^*$	8.271			0	79.0
24	3^1E_{2u}		$\sigma_8 \rightarrow \pi_3^*$	8.278			0	82.7
25	5^1E_{1g}	10	$\pi_2 \rightarrow 4d\sigma$	8.296			0	452.1
26	2^1B_{1g}	11	$\pi_2 \rightarrow 4d\sigma$	8.375			0	486.1
27	6^1E_{1g}	13	$\pi_2 \rightarrow 4d\sigma$	8.382			0	486.4
28	2^1B_{2g}	12	$\pi_2 \rightarrow 4d\sigma$	8.385			0	489.2
29	2^1E_{2g}		$\pi_2 \rightarrow 4d\pi$	8.497	8.44[g]	0.06	0	437.6
1	1^3B_{1u}		$\pi_2 \rightarrow \pi_3^*$	3.862	3.95[k]	−0.09	0	79.0
2	1^3E_{1u}		$\pi_2 \rightarrow \pi_3^*$	4.816	4.76[k]	0.06	0	79.7
3	1^3B_{2u}		$\pi_2 \rightarrow \pi_3^*$	5.689	5.60[k]	0.09	0	80.8
4	1^3E_{1g}	4	$\pi_2 \rightarrow 3s$	6.367	(6.33)[l]	(0.04)	0	126.3
5	1^3A_{2u}	5	$\pi_2 \rightarrow 3p\sigma$	6.876	(6.93)[l]	(−0.05)	0	146.7
6	1^3E_{2u}	6	$\pi_2 \rightarrow 3p\sigma$	7.003	(6.95)[l]	(0.05)	0	153.1
7	1^3A_{1u}	8	$\pi_2 \rightarrow 3p\sigma$	7.118			0	159.8
8	2^3E_{1u}	7	$\pi_2 \rightarrow 3p\pi$	7.132	(7.41, 7.19)[l]	(−0.28, −0.06)	0	148.9
9	2^3E_{1g}	10	$\pi_2 \rightarrow 3d\sigma$	7.420	(7.46)[l]	(−0.04)	0	137.3
10	1^3B_{2g}	12	$\pi_2 \rightarrow 3d\sigma$	7.576	(7.54)[l]	(0.04)	0	178.1
11	1^3E_{2g}		$\pi_1 \rightarrow \pi_3^*$	7.596	(7.49 ± 0.25)[j]	0.11	0	89.6
12	1^3B_{1g}	11	$\pi_2 \rightarrow 3d\sigma$	7.600	(7.54)[l]	(0.06)	0	181.6
13	3^3E_{1g}	13	$\pi_2 \rightarrow 3d\sigma$	7.604			0	181.4
14	1^3A_{1g}	15	$\pi_2 \rightarrow 3d\pi$	7.742	(7.80)[l]	(−0.06)	0	205.0
15	2^3E_{2g}	14	$\pi_2 \rightarrow 3d\pi$	7.832	(7.81)[l]	(0.02)	0	218.4
16	1^3A_{2g}	16	$\pi_2 \rightarrow 3d\pi$	7.863			0	241.2
17	4^3E_{1g}	17	$\pi_2 \rightarrow 4s$	7.960	(7.95)[l]	(0.01)	0	416.9
18	2^3A_{2u}	22	$\sigma_8 \rightarrow \pi_3^*$	8.002			0	79.8
19	2^3E_{2u}	24	$\sigma_8 \rightarrow \pi_3^*$	8.017			0	78.9
20	2^3A_{1u}	23	$\sigma_8 \rightarrow \pi_3^*$	8.040			0	78.3
21	3^3A_{2u}	18	$\pi_2 \rightarrow 4p\sigma$	8.123			0	468.7
22	3^3E_{2u}	19	$\pi_2 \rightarrow 4p\sigma$	8.156			0	479.7
23	3^3E_{1u}	21	$\pi_2 \rightarrow 4p\pi$	8.169	(8.37)[l]	(−0.20)	0	467.2
24	3^3A_{1u}	20	$\pi_2 \rightarrow 4p\pi$	8.188			0	490.7
25	5^3E_{1g}	25	$\pi_2 \rightarrow 4d\sigma$	8.270			0	452.6
26	2^3B_{2g}	28	$\pi_2 \rightarrow 4d\sigma$	8.366			0	487.7
27	6^3E_{1g}	27	$\pi_2 \rightarrow 4d\sigma$	8.373			0	486.0
28	2^3B_{1g}	26	$\pi_2 \rightarrow 4d\sigma$	8.374			0	486.1
29	2^3A_{1g}		$\pi_2 \rightarrow 4d\pi$	8.442	(8.44)[l]	(0.00)	0	453.2
30	3^3E_{2g}	29	$\pi_2 \rightarrow 4d\pi$	8.492	(8.44)[l]	(0.05)	0	438.5

https://doi.org/10.1021/acs.jctc.5c02112
J. Chem. Theory Comput. XXXX, XXX, XXX−XXX

Table 1. continued

No	State	Pair	Orbital picture	Ionization energy (IE) (eV)	Exptl. IE (eV)[m]	Δ(IE)	Intensity	Second moment (au)
1	1^2E_{1g}		$\pi_2 \rightarrow \infty$	9.226	9.45	−0.22	0.927	58.1
2	1^2E_{2g}		$\sigma_8 \rightarrow \infty$	12.103	(11.7)[n]		0.907	56.5
3	1^2A_{2u}		$\pi_1 \rightarrow \infty$	12.530	12.3	0.23	0.873	59.6
4	1^2E_{1u}		$\sigma_7 \rightarrow \infty$	14.347	14.47	−0.12	0.892	56.7
5	1^2B_{2u}		$\sigma_6 \rightarrow \infty$	14.780	14.78	0.00	0.881	59.3
6	1^2B_{1u}		$\sigma_5 \rightarrow \infty$	15.761	15.77	−0.01	0.880	55.1
7	1^2A_{1g}		$\sigma_4 \rightarrow \infty$	17.284	17.04	0.24	0.864	57.0

[a]Differences of excitation energies or ionization potentials between theory and experimental values. [b]Total energy (au) of the ground state, which is 165.016 kcal/mol higher than the estimated exact value of −232.248 au given in ref 50. [c]Ref 52. [d]Ref 53. [e]Ref 54. [f]Ref 55. [g]Refs 57 and 58. [h]Estimated using the Rydberg series formula. [i]Coefficients are mostly on π_2-3dπ and very small on π_1−π_3. [j]Ref 58. For the 1^3E_{2g} state, estimated in ref 62. [k]Ref 63. [l]Experimental data taken from those of corresponding singlet states. [m]Ref 64. [n]Noted as "approximate value" in ref 64.

Table 2. Total Energy of the Ground State of Benzene

Method	Hartree−Fock (HF) energy (au)	ΔE(HF)[a] (kcal/mol)	Correlation energy[b] (mH)	Total energy (au)	ΔE[c] (kcal/mol)
Blind challenge[51]					
ASCI	−230.721 819 131[b]	957.693	−860.0	−231.581 819	418.035
iCI			−861.1	−231.582 919	417.345
CCSDTQ			−862.4	−231.584 219	416.529
DMRG			−862.8	−231.584 619	416.278
FCCR			−863.0	−231.584 819	416.152
MBE-FCI			−863.0	−231.584 819	416.152
CAD-FCIQMC			−863.4	−231.585 219	415.901
AS-FCIQMC			−863.7	−231.585 519	415.713
SHCI			−864.2	−231.586 019	415.399
FC(SAC−CI, ESF) **theory**					
L2: Initial function + force	−230.434 344	1138.086	−848.1	−231.282 457	605.887
L3: FC(n = 1) + force	−230.728 099	953.752	−1165.6	−231.893 665	222.349
L4: FC(n = 2) + force	−230.760 102	933.670	−1201.2	−231.961 282	179.918
L5:FC(n = 2) + force + Ryd(3s,3p,3d)	−230.760 622	933.344	−1201.1	−231.961 721	179.643
L6: FC(n = 3) + force + Ryd(3s,3p,3d + 4s,4p,4d))	−230.771 455	926.546	−1213.6	−231.985 030	165.016
Estimated exact energy[50]	−232.248			−232.248	0

[a]Energy difference of the Hartree−Fock energy in kcal/mol from the estimated exact ground state energy of the benzene molecule. [b]For Blind Challenge, relative to the Hartree−Fock energy with the cc-pVDZ basis for all the methods. For the FC(SAC−CI, ESF) theory, relative to the Hartree−Fock energy at each level. [c]Energy difference of the total energies in kcal/mol from the estimated exact ground state energy of the benzene molecule.

even from crude initial functions. The other is that dimensions of basis functions soon increase as the order of the FC theory increases, and so we chose the smallest possible initial functions at the beginning. (4) At order 3 of final (L6) calculations, the MAE value showing the accuracy of the FC calculation became 0.095 eV = 2.2 kcal/mol, near the chemical accuracy.

In Figure 2, the present final result of the (L6) level is compared with previous SAC−CI results of 1987.[26] Though in the previous work we did our best to perform highly accurate calculations, the MAE value was 0.25 eV, in comparison with that of the present results, 0.095 eV. An important point of the present theory is that we can always improve toward the best possible result simply by applying the FC theory to higher orders. Further, another point is that we did not consider the effect of g_{ij} functions, which is the largest point which must be revisited in the future.

4. ACCURATE GROUND, EXCITED, AND IONIZED STATES OF BENZENE

Now, let us study electronic structures of the benzene molecule in its ground, excited, and ionized states at the present most accurate level, the final L6 level. Table 1 shows a summary of the present results obtained at the ground-state geometry. The results are compared with available experimental and theoretical data.[50−64] The table includes state assignments with orbital pictures, excitation or ionization energies, their experimental values, differences between theory and experiments, present theoretical oscillator strengths, and second moments. For the D_{6h} symmetry of benzene, oscillator strengths are zero except for $^1A_{2u}$ and $^1E_{1u}$ states. Even for these two symmetries, calculated oscillator strengths were very small for some states, and for such cases, values were recorded as 0.0 instead of 0. The second moment is a useful property indicating the size of the state, which is usually very different between the valence and Rydberg states.

Looking at columns showing differences between theoretical and experimental excitation energies, Δ(ExtE) and those for ionization energies, Δ(IE), we notice that these differences are generally very small across all states, confirming the high accuracy of the present theory. The second moment calculated for the ground state, 78.4 au, is the smallest of all the calculated values for singlet and triplet states, which is reasonable. Ionized states are all very slim and tight, as seen from values of second moments. This is because one excess positive charge around the

https://doi.org/10.1021/acs.jctc.5c02112
J. Chem. Theory Comput. XXXX, XXX, XXX−XXX

Table 3. Induced Electrostatic Forces Acting on Carbon and Hydrogen of Each Excited and Ionized State of Benzene at the Vertical Excited or Ionized State Fixed at the Ground-State Equilibrium Geometry, Due to the FC(SAC−CI, ESF) Theory at the L6 Level[a]

	State			Induced force acting on nucleus					
No	(D_{6h})	(d_{2h})	Orbital picture	$C_1(y)$	$H_1(y)$	$C_2(r)$	$C_2(\theta)$	$H_2(r)$	$H_2(\theta)$
2	1^1B_{2u}	1^1b_{3u}	$\pi_2 \rightarrow \pi_3^*$	0.033	−0.007				
3	1^1B_{1u}	1^1b_{2u}	$\pi_2 \rightarrow \pi_3^*$	0.024	−0.005				
4	1^1E_{1g}	1^1b_{2g}	$\pi_2 \rightarrow 3s$	0.018	0.001	0.051	−111	0.004	9
		1^1b_{3g}		0.018	0.005	0.051	−69	0.002	−18
5	1^1A_{2u}	1^1b_{1u}	$\pi_2 \rightarrow 3p\sigma$	0.021	0.003				
6	1^1E_{2u}	1^1a_u	$\pi_2 \rightarrow 3p\sigma$	0.023	0.002	0.023	0	0.003	4
		2^1b_{1u}		0.022	0.003	0.023	0	0.002	−5
7	1^1E_{1u}	2^1b_{2u}	$\pi_2 \rightarrow \pi_3^*, \pi_2 \rightarrow 3p\pi$	0.023	0.001	0.041	−59	0.002	4
		2^1b_{3u}		0.021	−0.003	0.041	58	0.000	−35
8	1^1A_{1u}	2^1a_u	$\pi_2 \rightarrow 3p\sigma$	0.025	0.002				
9	2^1E_{1u}	3^1b_{2u}	$\pi_2 \rightarrow 3p\pi, \pi_2 \rightarrow \pi_3^*$	0.017	−0.002	0.031	−17	0.003	19
		3^1b_{3u}		0.034	−0.003	0.023	23	0.002	−20
10	2^1E_{1g}	2^1b_{2g}	$\pi_2 \rightarrow 3d\sigma$	0.014	0.000	0.045	−108	0.005	−3
		2^1b_{3g}		0.014	0.006	0.045	−72	0.002	7
11	1^1B_{1g}	3^1b_{2g}	$\pi_2 \rightarrow 3d\sigma$	0.026	0.002				
12	1^1B_{2g}	3^1b_{3g}	$\pi_2 \rightarrow 3d\sigma$	0.026	0.003				
13	3^1E_{1g}	4^1b_{2g}	$\pi_2 \rightarrow 3d\sigma$	0.026	0.004	0.025	11	0.002	31
		4^1b_{3g}		0.024	0.001	0.026	−11	0.004	−19
14	1^1E_{2g}	3^1a_g	$\pi_1 \rightarrow \pi_3^*, \pi_2 \rightarrow 3d\pi$	0.021	0.001	0.021	0	0.001	−2
		1^1b_{1g}		0.021	0.001	0.021	0	0.001	2
15	2^1A_{1g}	2^1a_g	$\pi_2 \rightarrow 3d\pi$	0.021	0.001				
16	1^1A_{2g}	2^1b_{1g}	$\pi_2 \rightarrow 3d\pi$	0.022	0.002				
17	4^1E_{1g}	5^1b_{2g}	$\pi_2 \rightarrow 4s$	0.020	0.001	0.051	−114	0.003	15
		5^1b_{3g}		0.021	0.004	0.051	−66	0.002	−28
18	2^1A_{2u}	3^1b_{1u}	$\pi_2 \rightarrow 4p\sigma$	0.021	0.002				
19	2^1E_{2u}	3^1a_u	$\pi_2 \rightarrow 4p\sigma$	0.022	0.002	0.022	0	0.002	3
		4^1b_{1u}		0.022	0.002	0.022	0	0.002	−3
20	2^1A_{1u}	4^1a_u	$\pi_2 \rightarrow 4p\sigma$	0.023	0.002				
21	3^1E_{1u}	4^1b_{2u}	$\pi_2 \rightarrow 4p\pi$	0.021	0.003	0.050	−66	0.001	−55
		4^1b_{3u}		0.020	0.000	0.050	−114	0.002	24
22	2^1A_{2u}	11^1b_{1u}	$\sigma_8 \rightarrow \pi_3^*$	0.002	0.003				
23	3^1A_{1u}	9^1a_u	$\sigma_8 \rightarrow \pi_3^*$	0.004	0.001				
24	3^1E_{2u}	10^1a_u	$\sigma_8 \rightarrow \pi_3^*$	0.004	0.002	0.003	27	0.003	−2
		10^1b_{1u}		0.003	0.003	0.004	−23	0.002	3
25	5^1E_{1g}	6^1b_{2g}	$\pi_2 \rightarrow 4d\sigma$	0.018	0.001	0.050	−112	0.003	11
		6^1b_{3g}		0.019	0.004	0.049	−68	0.002	−23
26	2^1B_{1g}	7^1b_{2g}	$\pi_2 \rightarrow 4d\sigma$	0.024	0.002				
27	6^1E_{1g}	8^1b_{2g}	$\pi_2 \rightarrow 4d\sigma$	0.024	0.002	0.023	3	0.002	10
		8^1b_{3g}		0.023	0.002	0.024	−3	0.002	−8
28	2^1B_{2g}	7^1b_{3g}	$\pi_2 \rightarrow 4d\sigma$	0.024	0.002				
29	2^1E_{2g}	5^1a_g	$\pi_2 \rightarrow 4d\pi$	0.022	0.001	0.021	−1	0.001	−2
		3^1b_{1g}		0.021	0.001	0.022	1	0.001	2
1	1^3B_{1u}	1^3b_{2u}	$\pi_2 \rightarrow \pi_3^*$	0.025	−0.007				
2	1^3E_{1u}	2^3b_{2u}	$\pi_2 \rightarrow \pi_3^*$	0.030	−0.007	0.027	−2	0.007	1
		1^3b_{3u}		0.026	−0.007	0.029	2	0.007	−1
3	1^3B_{2u}	2^3b_{3u}	$\pi_2 \rightarrow \pi_3^*$	0.023	−0.006				
4	1^3E_{1g}	1^3b_{2g}	$\pi_2 \rightarrow 3s$	0.017	0.001	0.050	−110	0.004	8
		1^3b_{3g}		0.017	0.005	0.050	−70	0.002	−17
5	1^3A_{2u}	1^3b_{1u}	$\pi_2 \rightarrow 3p\sigma$	0.020	0.002				
6	1^3E_{2u}	1^3a_u	$\pi_2 \rightarrow 3p\sigma$	0.023	0.002	0.022	0	0.003	5
		2^3b_{1u}		0.022	0.003	0.023	0	0.002	−6
7	1^3A_{1u}	2^3a_u	$\pi_2 \rightarrow 3p\sigma$	0.024	0.002				
8	2^3E_{1u}	3^3b_{2u}	$\pi_2 \rightarrow 3p\pi$	0.018	0.002	0.050	−70	0.001	−112
		3^3b_{3u}		0.017	−0.001	0.050	−111	0.001	31
9	2^3E_{1g}	2^3b_{2g}	$\pi_2 \rightarrow 3d\sigma$	0.011	0.000	0.045	−105	0.005	−4
		2^3b_{3g}		0.012	0.007	0.045	−75	0.002	9
10	1^3B_{2g}	3^3b_{3g}	$\pi_2 \rightarrow 3d\sigma$	0.026	0.003				

https://doi.org/10.1021/acs.jctc.5c02112
J. Chem. Theory Comput. XXXX, XXX, XXX−XXX

Table 3. continued

No	State (D_{6h})	(d_{2h})	Orbital picture	Induced force acting on nucleus $C_1(y)$	$H_1(y)$	$C_2(r)$	$C_2(\theta)$	$H_2(r)$	$H_2(\theta)$
11	1^3E_{2g}	1^3a_g	$\pi_1 \to \pi_3$*	0.063	−0.007	0.052	−44	0.006	10
		1^3b_{1g}		0.029	−0.005	0.066	33	0.007	−9
12	1^3B_{1g}	3^3b_{2g}	$\pi_2 \to 3d\sigma$	0.026	0.002				
13	3^3E_{1g}	4^3b_{2g}	$\pi_2 \to 3d\sigma$	0.026	0.004	0.025	9	0.002	29
		4^3b_{3g}		0.024	0.001	0.026	−9	0.004	−18
14	1^3A_{1g}	2^3a_g	$\pi_2 \to 3d\pi$	0.020	0.001				
15	2^3E_{2g}	3^3a_g	$\pi_2 \to 3d\pi$	0.026	0.001	0.023	−8	0.001	−13
		3^3b_{1g}		0.022	0.000	0.025	8	0.001	9
16	1^3A_{2g}	2^3b_{1g}	$\pi_2 \to 3d\pi$	0.022	0.001				
17	4^3E_{1g}	5^3b_{2g}	$\pi_2 \to 4s$	0.020	0.001	0.051	−114	0.003	15
		5^3b_{3g}		0.021	0.004	0.051	−66	0.002	−27
18	2^3A_{2u}	9^3b_{1u}	$\sigma_8 \to \pi_3$*	0.001	0.003				
19	2^3E_{2u}	10^3a_u	$\sigma_8 \to \pi_3$*	0.005	0.000	0.003	45	0.003	−13
		10^3b_{1u}		0.001	0.003	0.004	−25	0.001	29
20	2^3A_{1u}	9^3a_u	$\sigma_8 \to \pi_3$*	0.007	0.000				
21	3^3A_{2u}	3^3b_{1u}	$\pi_2 \to 4p\sigma$	0.021	0.002				
22	3^3E_{2u}	3^3a_u	$\pi_2 \to 4p\sigma$	0.022	0.002	0.022	0	0.002	4
		4^3b_{1u}		0.022	0.002	0.022	0	0.002	−4
23	3^3E_{1u}	4^3b_{2u}	$\pi_2 \to 4p\pi$	0.021	0.003	0.051	−66	0.001	−56
		4^3b_{3u}		0.020	0.000	0.051	−114	0.002	22
24	3^3A_{1u}	4^3a_u	$\pi_2 \to 4p\pi$	0.023	0.002				
25	5^3E_{1g}	6^3b_{2g}	$\pi_2 \to 4d\sigma$	0.018	0.001	0.049	−113	0.003	10
		6^3b_{3g}		0.019	0.004	0.049	−68	0.002	−21
26	2^3B_{2g}	7^3b_{3g}	$\pi_2 \to 4d\sigma$	0.023	0.002				
27	6^3E_{1g}	8^3b_{2g}	$\pi_2 \to 4d\sigma$	0.024	0.002	0.023	4	0.002	11
		8^3b_{3g}		0.023	0.002	0.024	−4	0.002	−9
28	2^3B_{1g}	7^3b_{2g}	$\pi_2 \to 4d\sigma$	0.024	0.002				
29	2^3A_{1g}	4^3a_g	$\pi_2 \to 4d\pi$	0.020	0.001				
30	3^3E_{2g}	5^3a_g	$\pi_2 \to 4d\pi$	0.021	0.001	0.021	−1	0.001	−2
		4^3b_{1g}		0.021	0.001	0.021	1	0.001	2
1	1^2E_{1g}	1^2b_{2g}	$\pi_2 \to \infty$	0.021	0.000	0.052	−116	0.002	19
		1^2b_{3g}		0.023	0.003	0.052	−65	0.001	−41
2	1^2E_{2g}	1^2a_g	$\sigma_8 \to \infty$	−0.072	0.024	0.071	57	0.014	−51
		1^2b_{1g}		0.075	0.003	0.069	59	0.022	30
3	1^2A_{2u}	1^2b_{1u}	$\pi_1 \to \infty$	0.055	0.004				
4	1^2E_{1u}	1^2b_{2u}	$\sigma_7 \to \infty$	−0.029	0.032	0.061	−55	0.009	−2
		1^2b_{3u}		0.056	0.002	0.051	−81	0.024	1
5	1^2B_{2u}	2^2b_{3u}	$\sigma_6 \to \infty$	0.059	0.008				
6	1^2B_{1u}	2^2b_{2u}	$\sigma_5 \to \infty$	−0.053	0.031				
7	1^2A_{1g}	2^2a_g	$\sigma_4 \to \infty$	0.021	0.023				

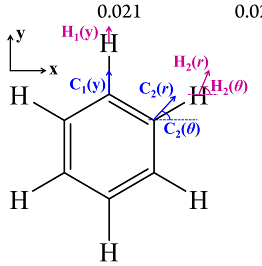

[a] A figure of a benzene molecule showing definitions of some quantities used in this table.

nuclear framework pulls all surrounding electron clouds toward itself.

In the first row of Table 1, the ground state energy calculated with this theory is given. It is −231.985 030 au, which is 165.016 kcal/mol higher than the estimated exact value of −232.248 au[50] This deviation is because the present SAC calculation was limited to include only up to singles-and-doubles-linked excitation operators within the usage of g_{iA}-type scaling functions of the FC calculations. However, to solve this problem, the inclusion of g_{ij}-type scaling functions would be most straightforward, but this is a subject for the future.

In 2020, essentially full CI, but frozen-core, ground-state energy of benzene was calculated with the cc-pVDZ basis, using many different sophisticated theories of many authors.[51] In Table 2, we referred to their results[51] as "blind challenge" data, together with the present result obtained at different levels. The blind challenge data are essentially full-CI frozen-core data, and so the results of different methods are close to each other. On the

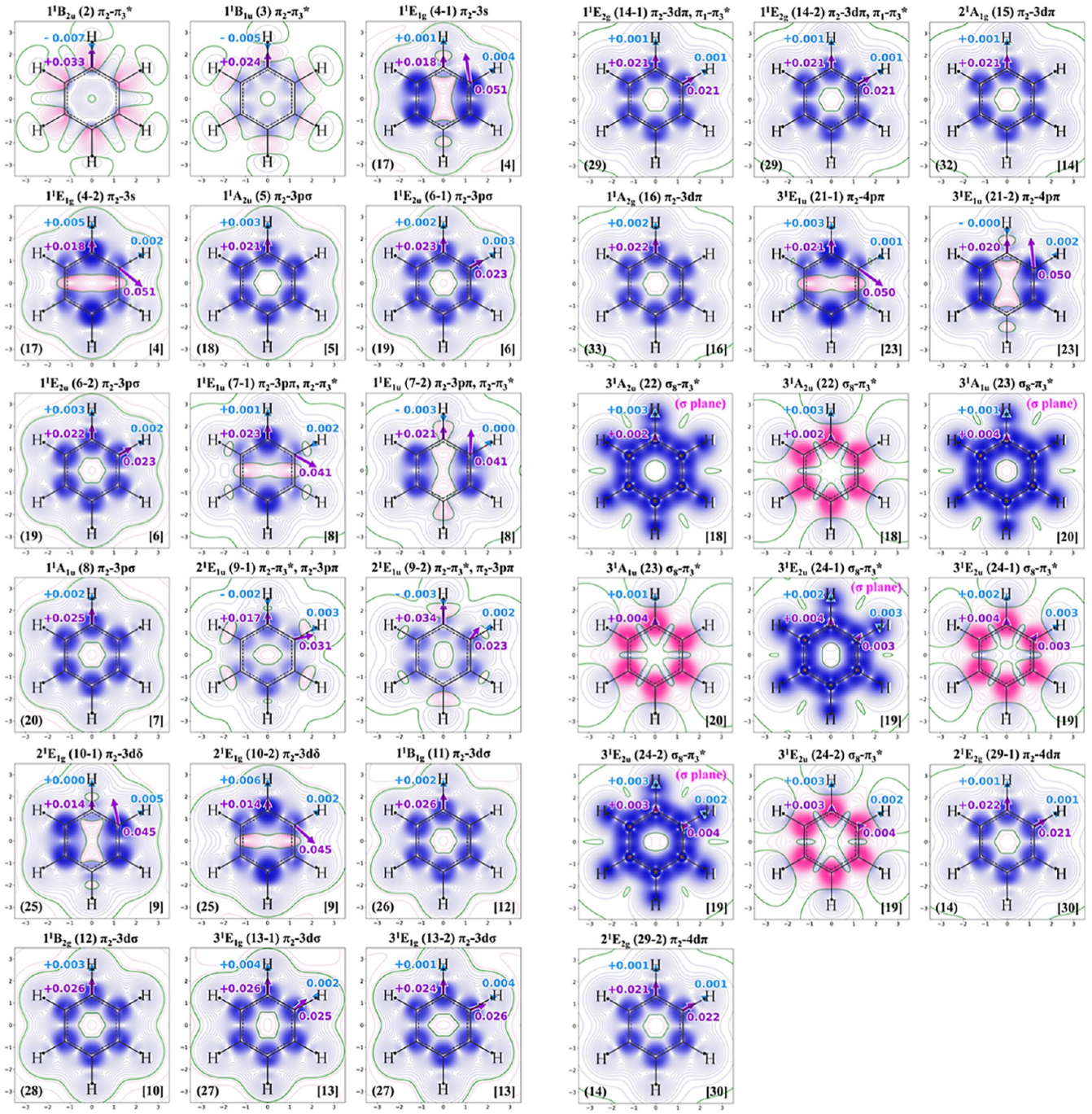

Figure 3. Force and density difference maps for singlet excited states of benzene given in Table 1. For the state to which the map is very similar, the singlet pair number is given on the lower left corner, and the triplet pair number is given on the lower right corner. Green, red, and blue lines mean zero, plus, and minus, respectively. Most maps are on the plane 1 au above the benzene plane and when necessary, the map on the molecular plane is also given, marked as the σ plane.

other hand, the present result given in Table 2 is the ground-state data at several different levels of the present theory shown in Figure 1. As the order of the FC theory is raised, the ground-state energy becomes lower. The addition of Rydberg functions gives only a small effect on the ground state energy. In the present calculation, the "correlation energy" was given relative to the Hartree−Fock energy at each level of calculations. Note that, even with increasing the order of the FC theory, the Hartree−Fock energy "saturates" at some level, but the energy of the present theory is improved systematically toward the exact solution by increasing the order of the theory. However, even at the L6 level, the ground state energy differs from the exact energy by 165.016 kcal/mol. As stated above, this is because the present calculation does not include g_{ij} functions and is limited to only single and double excitation-level in SAC calculations. Since these approximations are popular in conventional quantum chemistry, they would not be so critical.

We now move to the excited states. From the second row of Table 1, all data are for excited and ionized states at their vertical geometry of the ground state. The excitation energy is a difference quantity between ground and excited states, and therefore, it would be more stable than two absolute energy

https://doi.org/10.1021/acs.jctc.5c02112
J. Chem. Theory Comput. XXXX, XXX, XXX−XXX

values. At the vertical excited or ionized state, each nucleus of the molecule will receive the force that works to move it toward the position of the equilibrium geometry of each state because the equilibrium geometry of each state will be different from the ground-state one. In Table 3, the Hellmann−Feynman forces acting on carbon and hydrogen atoms of the benzene molecule at vertical states are summarized as induced forces. The present theory is designed so that not only the energy but also the force acting on each nucleus is highly accurate, and the latter can be easily calculated using the ESF theorem when the wave function is calculated to be "stable" using derivative bases that are added and also as the order of the present theory is increased. Since the ESF is calculated from the one-electron density, forces induced at vertical excited and ionized states are calculated only with the deference density $\Delta\rho$ defined by $\Delta\rho = \rho_{ex,ion} - \rho_{ground}$, where $\rho_{ex,ion}$ is the electron density of the excited or ionized state, and ρ_{ground} is the electron density of the ground state. This difference quantity is considered to be more accurate than the density itself because of the cancellation of errors. Further, the ESF has simple and visual force concepts.[36−46] With this simplicity and visuality, understanding and even the prediction of chemical phenomena would become easier and more transparent.

The density difference maps with induced forces acting on carbon and hydrogen nuclei are given in Figure 3 for singlet states, Figure 4 for triplet states, and Figure 5 for ionized states, and the induced force data are given in Table 3 for all states. In SAC−CI calculations, the benzene molecule was actually dealt with in the D_{2h} symmetry as the Abelian subgroup of D_{6h}. For degenerate states, we gave the result for each of two symmetry members using the symmetry symbol of the D_{2h} symmetry with a noncapital letter. Density difference maps are given mostly on the plane 1 au above the benzene plane because most excitations occur in the domain of π electrons. For the change in the σ domain, the density difference on the benzene plane was given and noted with "(σ plane)". Two elements of degenerate symmetry are written as k-1 and k-2 with k being the number of the degenerate state. In contour plots of density difference maps, the red color shows an increase in density and blue a decrease caused by excitation or ionization, and green shows the zero line. The contour plots are generated with the range of 0.002 to 0.002 divided by 1000. Induced forces are shown by arrows starting from a carbon or hydrogen nucleus.

Here, we deal with many excited states: in exact theory, each state is as important as the ground state. However, it is difficult to present all of their density-difference maps due to space limitations. So, we examined all maps and found that much similarity exists, particularly for Rydberg-excited states between those for 3s, 3p, and 3d Rydberg excitations and 4s, 4p, and 4d Rydberg excitations. This is because the Rydberg orbitals are much outside the molecule, and therefore, maps of only around the benzene nuclear skeleton are similar between third-period and fourth-period excitations. Using this fact, we could skip maps for 4-th period Rydberg excitations by giving their state number, defined in Table 1 on the lower left corner of each map of the third-period Rydberg excitation. Further, maps of triplet Rydberg excitation are also very similar to corresponding singlet counter maps. So, we showed in the lower right corner of the singlet map the number of the triplet counterpart defined in Table 1. On the contrary, in maps for triplet states, we gave the corresponding singlet pair number on the lower right corner of the triplet map. In this way, we could make the number of maps shown on this paper be the minimum possible. However, all the original maps are certainly necessary and therefore summarized in Supplemental Figures S1 and S2, because "similarity" is not an absolute measure and we need all genuine maps for detailed examinations. Thus, Figures S1 and S2 in the Supporting Information give all genuine maps for singlet and triplet states. Figures 3 and 4 of this text show only selected maps for singlet and triplet states, respectively. For singlet maps, singlet pair numbers are given on lower left corners and triplet pair numbers on lower right corners. For triplet maps, singlet pair numbers are given in lower right corners. For an ionized state, no pairing maps exist.

4.1. Singlet Excited States

Now, let us examine singlet excited states from both energy and force concepts. Table 1 shows the energetics compared with experiments,[52−64] oscillator strengths, and second moments for 28 singlet excited states. Table 3 summarizes the details of induced forces acting on the carbon and hydrogen nuclei of these states. Figure 3 shows density difference maps that cause induced forces as shown. Though all data are given in Figure S1 of the Supporting Information, we have to limit the number of maps for a space reason: Figure 3 shows force and density difference maps for the lower 22 states. For 6 states not shown, we explained their results by referring to the maps within 22 states that resemble very much. All force values are given in Table 3. Now, let us examine each state in the order of the energy.

The lowest two excited states are 1^1B_{2u} (No. 2) and 1^1B_{1u} (No. 3), $\pi_2-\pi_3^*$ valence states from degenerate homo's to lumo's. Their second moments, 79.9 and 82.5 au, are very close to each other and a bit larger than that of the ground state, 77.4 au. These two states are symmetry forbidden. In experimental UV spectra for the gas phase shown by Dawes et al.,[56] very weak peaks exist at around 4.90 eV, which were assigned to the 1^1B_{2u} state, and stronger peaks at around 6.2 eV were assigned to the 1^1B_{1u} state. These assignments are the same as those by Lassettre et al.[52] The first two diagrams of Figure 3 show density difference maps and the induced forces for 1^1B_{2u} (No. 2) and 1^1B_{1u} (No. 3) states. We see a decrease of the π electron density from the C−C bond region, which causes the force acting on C of +0.033 and +0.024 au, respectively, both working to increase C−C distances. On the other hand, the forces acting on H are −0.007 and −0.005 au, respectively, working to decrease H−C distances.

Next, we examine three Rydberg states, 1^1E_{1g} (No. 4), 1^1A_{2u} (No. 5), and 1^1E_{2u} (No. 6) calculated at 6.421(3s), 6.945(3pσ), and 7.019(3pσ) eV, respectively, as assigned experimentally by Johnson et al.[53,54] as 6.33, 6.93, and 6.95 eV, respectively. They arise by excitations from degenerate π_2 orbitals to Rydberg 3s and 3pσ orbitals. Though the 1^1A_{2u} (No. 5) ($\pi_2 \rightarrow$ 3pσ) state is symmetry allowed (oscillator strength of 0.087), its peak at around 7 eV is in the region of strong absorption peaks due to two $^1E_{1u}$ states (oscillator strengths of 0.468 and 0.514) are explained below. As seen from Figure 3, in 1^1A_{2u} (No. 5) Rydberg excited state, the electron density decrease is seen almost everywhere in the molecular region on the plane 1 au above the molecular plane. Rydberg orbitals are largely outside the molecular region, as seen from the density increase region (shown in red), apart from six H atoms. Note that the green line is the zero line that divides decrease and increase regions, and the positive region shown outside in red is the region of the 3p Rydberg orbitals. Then, all bonds will be elongated in these excited states as seen from positive forces acting on carbons. It is interesting to compare two degenerate E states, Nos. 4 and 6,

https://doi.org/10.1021/acs.jctc.5c02112
J. Chem. Theory Comput. XXXX, XXX, XXX−XXX

lower and higher states of the 1^1A_{2u} (No. 5) ($\pi_2 \rightarrow 3p\sigma$) state explained above. In the 1^1E_{1g} (No. 4) ($\pi_2 \rightarrow 3s$) state, maps of degenerate two states are different, but in the 1^1E_{2u} (No. 6) ($\pi_2 \rightarrow 3p\sigma$) state, maps of degenerate two states are almost the same. Then, in the lower 1^1E_{1g} (No. 4) state, the Jahn−Teller distortion would occur, but in the upper 1^1E_{2u} (No. 6) ($\pi_2 \rightarrow 3p\sigma$) state, such distortion would not occur.

Very closely to the above 1^1E_{2u} (No. 6) peak, two $^1E_{1u}$ states (Nos. 7 and 9), which are very important excited states of benzene among many states, were calculated at 7.089 eV (No. 7) and 7.386 eV (No. 9), together with the 1^1A_{1u} state (No. 8) at 7.112 eV. Among these, two $^1E_{1u}$ states are strongly symmetry-allowed, and their oscillator strengths were as large as 0.468 and 0.514, respectively. They thus give very strong overlapping peaks in experimental VUV spectra, as shown by Dawes et al.[56] Though the 1^1E_{2u} (No. 6) state was pure Rydberg, the present two $^1E_{1u}$ states are mixed valence $\pi_2-\pi_3$* and Rydberg $\pi_2-3p\pi$ states. This mixing is special to the singlet states, as will be clear later in the triplet part, and this is a reason why these two $^1E_{2u}$ states are here at the very close energy region of 7.09−7.39 eV. In other words, in comparison with the triplet state, the valence singlet $^1E_{2u}$ state is higher by about twice the exchange integral between π_2 and π_3*MO's. As a result, roughly speaking, this valence $^1E_{2u}$ state could mix with the nearby second Rydberg $^1E_{2u}$ state. As expected from the magnitude of the oscillator strength, the valence character is smaller in the first 1^1E_{1u} state than that in the second 2^1E_{1u} state. This is also seen from the magnitudes of their second moments, 126.9 au and 116.5 au, respectively. In the experimental VUV spectra,[56] present two $^1E_{1u}$ states give a very strong broad VUV peak in the 6.7−7.5 eV region. For the 1^1E_{1u} (No. 7) state, 6.95 eV was assigned in the earlier paper.[52] For the 2^1E_{1u} (No. 9) state, both 7.41 eV[55] and 7.19 eV[57,58] data existed, but the former is closer to our calculated excitation energy. In Figure 3, force and density maps of two $^1E_{1u}$ (Nos. 7 and 9) states and the 1^1A_{1u} state are shown. Because these two $^1E_{1u}$ states are mixed valence-Rydberg, positive valence density regions are seen for the 1^1E_{1u} (No. 7) state, and for the 2^1E_{1u} (No. 9) state, the negative density is much shallower in the benzene region in comparison with pure Rydberg states like 1^1A_{1u} (No. 8) and even in comparison with 1^1E_{1u} (No. 7) shown in Figure 3. Also, a strong Jahn−Teller distortion is expected for the first 1^1E_{1u} state, but such a distortion would be mild in the second 1^1E_{1u} state. The presence of these two $1-2^1E_{1u}$ states at this close energy region, 7.089 and 7.386 eV, in contrast to 4.816 and 7.132 eV of triplet $1-2^3E_{1u}$ state, is characteristic for the photochemistry of the singlet excited states of benzene.

The next four states, 2^1E_{1g}, 1^1B_{1g}, 1^1B_{2g}, and 3^1E_{1g} (No. 10−13) are all 3d Rydberg in character, as seen from Table 1 and Figure 3. They are very close to each other in energy, lying within 7.496−7.622 eV, only 0.126 eV separation. Earlier studies[52,53] remarked the ambiguity in assignments of these states. Based on the present reliable results of the excitation energy, we assign observed peaks at 7.46 and 7.54 eV as follows: the 2^1E_{1g} state calculated at 7.496 eV is assigned to the peak at 7.46 eV estimated by us[26] and the 1^1B_{1g} and 1^1B_{2g} states calculated at 7.603 and 7.613 eV to two peaks observed at 7.54 eV by Whetten and others.[57] The last 3^1E_{1g} state does not have an observed counterpart. Because these are all Rydberg states and their intensities (oscillator strength) are all zero, the assignment is essentially difficult. Note that present assignments differ from previous ones.[26] Density difference maps of these four states, 2^1E_{1g}, 1^1B_{1g}, 1^1B_{2g}, and 3^1E_{1g} (No. 10−13), are shown in Figure 3. All are typical Rydberg types: densities in the valence region are all negative, showing the loss of an electron from the valence π_2 orbital region and adding one electron on the Rydberg 3d orbital region that lies outside of the benzene valence region. Further, we expect that for the first degenerate 2^1E_{1g} (No. 10) state, the Jahn−Teller distortion would occur in the reorganization process, while such distortion is not expected for the 3^1E_{1g} state. Geometrical changes of three 1^1B_{1g}, 1^1B_{2g}, and 3^1E_{1g} (No. 11−13) states would be similar: forces acting on C and H nuclei are also very similar among these three states.

Let us examine an important state, 1^1E_{2g} (No. 14), which is very interesting from a theoretical point of view, because this state was expected before to be the valence $\pi_1-\pi_3$* state. This and higher valence excited states were difficult before[26] with the previous SAC−CI alone theory and calculations, but here with the advanced exact SAC−CI formalism, FC, or SSE(SAC−CI, ESF) theory, we obtained results shown in Table 1 and Figure 3. From these results, it turned out that the valence $\pi_1-\pi_3$* nature is very small, and it is mostly Rydberg π_2-3dπ state whose second moment is as large as 228.3 au. The calculated excitation energy was 7.822 eV, which is very close to the experimental value, 7.81 eV by Whetten et al.[57,58] and 7.8 eV by Yoshihara et al.[59−61] This state is doubly degenerate, but the two components shown in Figure 3 have essentially the same density profile, showing that no Jahn-teller distortion will occur in this excited state. These two density profiles are very similar to those of previous 1^1B_{1g} (No. 11) and 1^1B_{2g} (No. 12) states, though their second moments were smaller at 182−185 au. They are also similar to the next two states, 2^1A_{1g} (No. 15)[57] and 1^1A_{2g} (No. 16), which are Rydberg π_2-3dπ states, whose second moments are also very similar, 238.5 au and 240.8 au, respectively. Their density profiles, which are for the nondegenerate states, are also very similar to those of the 1^1E_{2g} (No. 14) state, which are degenerate.

The states from No. 17 to No. 21 are a set of Rydberg states arising from π_2 to the outer Rydberg 4s and 4p orbitals. The first state, 4^1E_{1g} (No. 17), π_2-4s is at 7.971 eV, and the next three states, 2^1A_{2u} (No. 18), 2^1E_{2u} (No. 19), and 2^1A_{1u} (No. 20) are π_2-4pσ excitations, and the last 3^1E_{1u} (No. 21) is π_2-4pπ. Therefore, their second moments are so large, exceeding 400 au and even close to 500 au. Among them, 2^1A_{2u} (No. 18) and 3^1E_{1u} (No. 21) are symmetry-allowed states, which are calculated to be 8.141 and 8.193 eV, respectively. Their energy separation is as small as 0.052 eV, and their oscillator strengths are small, as calculated to be 0.018 and 0.000 au, respectively. On the other hand, experimentally, there are two observed peaks at 7.95 eV[57] and 8.37 eV.[55] We assign the peak observed at 7.95 eV to 4^1E_{1g} (No. 17) as Whetten, Grubb et al.[57,58] did based on the two- and four-photon absorption spectroscopy that observes states whose symmetries are E_{1g}, E_{2g}, A_{1g}, and A_{2g} symmetries. The observed peak at 8.37 eV is assigned to state 3^1E_{1u} (No. 21) calculated at 8.193 eV. These assignments are the same as those made in our previous SAC−CI study. We note that density difference maps of present states No. 17 to No. 21 are very similar to corresponding ones from π_2 to Rydberg 3s, 3p orbitals shown above already in Figure 3, namely between pairs, Nos. 17 and 4, 18 and 5, 19 and 6, 20 and 8, and 21 and 7. Therefore, though, all density difference maps are given in Supplemental Figure S1, we skip them in Figure 3 of this text, except for the last state, 3^1E_{1u} (No. 21), for which the force and difference density map is given in Figure 3. The reasons are as follows. First, states1^1E_{1u} (No. 7) and 2^1E_{1u} (No. 9) are, as we already examined above, very important symmetry-allowed states observed in the UV

https://doi.org/10.1021/acs.jctc.5c02112
J. Chem. Theory Comput. XXXX, XXX, XXX−XXX

spectra.[52−61] Second, the lower two states, 1^1E_{1u} (No. 7) and 2^1E_{1u} (No. 9), were both valence-Rydberg mixed states, as shown in Table 1. Therefore, it is very interesting to study whether the mixing between valence and Rydberg states occurs in the 3^1E_{1u} (21) state. It is found from the present calculations that the main configuration of the 3^1E_{1u} (21) state is dominantly π_2-4pπ, and the mixing with the valence is very slight. This is supported by the large second moment of 465.8 au shown in Table 1. This is also seen from the force and difference density map of this state shown in Figure 3, which is similar to the maps of 1^1E_{1g} (4) π_2-3s and 2^1E_{1g} (10) π_2-3dδ, both being typical Rydberg transitions. From Table 3, we can check a similarity or difference of the induced forces among this state against π_2-3s, 3p, No. 4−6, and π_2-4s, 4p, No. 17−21, and find that though for π_2-3s alone, the force acting on carbon is slightly smaller, others are all around 0.021−0.023 au and similar. Anyway, these three $^1E_{1u}$ states, Nos. 7, 9, and 21 states, are all unique in singlet excited states of benzene. In triplet states, the situation will be different.

Then, three valence states, No. 22−No. 24, 3^1A_{2u}, 3^1A_{1u}, and 3^1E_{2u} follow. They lie very close to each other at 8.208, 8.271, and 8.278 eV, only with a 0.07 eV width, and the latter two are so close to each other. The first state, No. 22 3^1A_{2u}, is symmetry allowed. These three states are new valence states arising by excitations from occupied degenerate σ_8 orbitals to outer degenerate π_3* orbitals, both being valence orbitals. Therefore, in Figure 3, two sets of maps of σ and π regions are shown for these states. The σ region is on the benzene plane, and the π region is 1 au above the benzene plane. From Table 1, the oscillator strength of the first symmetry-allowed state No. 22 is 0.006, a weak transition. The other two transitions, 3^1A_{1u} (No. 23) and 3^1E_{2u} (No. 24), are symmetry forbidden. The second moments are all very small as valence states. In particular, the second 3^1A_{1u} state is tight, 79.0, which is close to 78.4, the ground-state value. In Figure 3, difference density maps of these three states are shown. They are certainly typical valence types. Looking at three σ maps of Nos. 22, 23, and 24, we notice that they are very similar, almost the same. However, three maps on the π plane are not the same, though similar. Theoretically speaking, main configurations are all σ_8−π_3*, but their detailed SAC−CI coefficients are different. Common to this result is a decrease in the σ_8 region and an increase in the π_3* region. The induced forces (Table 3) are similar and small, particularly on carbon. In the last state 3^1E_{2u} No. 24, two degenerate states are also similar, indicating that the extent of the Jahn−Teller distortion would be small.

From Nos. 25 to 29, these five states are due to Rydberg transitions from degenerate π_2 orbitals to Rydberg 4d orbitals. Because both 3d and 4d Rydberg orbitals are much outside of the valence region, density difference maps around the valence region are similar between those having the same symmetry designation, as confirmed from Figure S1 of the Supporting Information, and so the difference density maps of No. 25 to No. 28 were omitted here. Their energy width is interesting: the first four are very close and lie within the width of 0.089 eV, but the last one, No. 29 2^1E_{2g}, π_2-4dπ lies at 8.497 eV, 0.112 eV above the state 2^1B_{2g}. Further, among these five transitions, only this state was assigned to the experimentally observed peak[57,58] at 8.44 eV. This state is actually the second state of the same symmetry of the earlier important state 1^1E_{2g} (No. 14), which was the Rydberg-valence mixed state observed at 7.80−7.81 eV, as stated above. Because these five states are transitions to Rydberg 4d orbitals, their second moments are as large as 437−489 au in comparison with those of 3d Rydberg transitions No. 10−No. 16 of 146−241 au. Among them, the second moment of the No.29 2^1E_{2g} state alone is small, implying some small valence-state mixing. Actually, a small contribution of the valence π_1−π_3* transition was confirmed from the SAC−CI output, similar to the lower 1^1E_{2g} state studied above in some details. For this reason, we showed the density difference maps of this state as the last pair of figures of Figure 3. Actually, their figures are certainly very close to those of the 1^1E_{2g} state studied above: valence mixing is very small, induced forces acting on C and H nuclei are similar, and Jahn−Teller distortion would not occur. Though there are still many excited states higher until below the first ionization level, 9.45 eV, the examination of the singlet vertical excited states is stopped here because we added Rydberg bases only up to the 4s, 4p, and 4d levels.

4.2. Triplet Excited States

Next, the triplet excited states of benzene are studied with the present theory. In Table 1, results for triplet states are also summarized in comparison with experimental data.[62,63] Generally speaking, triplet states are difficult to observe because they are forbidden by spin symmetry. However, for triplet Rydberg excitations, we estimated experimental values from corresponding singlet excitation values because for Rydberg excitations, the singlet−triplet difference of the excitation energy should be small. We also note the same similarity in density difference maps for triplet states. Though full data of density difference maps for 30 triplet states are given in Figure S2 of the Supporting Information, the data in this paper shown in Figure 4 is limited only to the first three valence excited states, Nos. 1−3, 1^3B_{1u}, 1^3E_{1u}, and 1^3B_{2u}, and a higher valence excited state No. 11 1^3E_{2g}. Additionally, the data for 2^3E_{2g} and 3^3E_{2g} states were also given in Figure 4 for their importance. For others, triplet data are similar to the corresponding singlet ones.

The first three states (No. 1−3), 1^3B_{1u}, 1^3E_{1u}, and 1^3B_{2u} are π_2−π_3* excited triplet states that are genuine valence states as seen from their small second moments of 79−81 au. These three triplet states were studied experimentally,[56,63] and their excitation energies agree well with present theoretical values to within 0.1 eV, as seen from Table 1. Among them, the 1^3E_{1u} state is unique. In the triplet, its energy is 4.816 eV, while in the singlet, it was 7.089 eV. This difference of 2.27 eV is partially from the exchange integral between π_2 and π_3* MO's, which is large between these valence MO's. Because of this big energy difference, triplet 1^3E_{1u} could be a pure valence state without mixing of the Rydberg 2^3E_{1u} state, No. 8, lying at 7.132 eV. In Figure 4, density difference maps with forces are shown. The map of the 1^3B_{1u} state is very similar to that of the 1^1B_{2u} state: both are π_2−π_3* state. The present two 1^3E_{1u} states (2−1 and 2−2) in Figure 4 are also similar to the 1^1B_{2u} state, both are again the π_2−π_3* state. However, in comparison with the singlet 1^1E_{1u} (7−1 and 7−2) states shown in Figure 3, maps of the corresponding triplet 1^3E_{1u} states are quite different: singlet ones are Rydberg-valence mixed states, but triplet ones are uniquely pure valence π_2−π_3* type and so similar to the map of the first 1^3B_{1u} state and more closely to the map of the singlet 1^1B_{2u} (2) of Figure 3. Also, maps of 1^3B_{2u} (3) and 1^1B_{1u} (3) are similar, and both are valence states, but higher ones have smaller spaces of positive density on the benzene ring region. For the 1^3E_{1u} (No. 2) state, two maps of the degenerate state are very similar, and so the Jahn−Teller distortion will not occur. From the force data, we expect that the C−C bond will be elongated

https://doi.org/10.1021/acs.jctc.5c02112
J. Chem. Theory Comput. XXXX, XXX, XXX−XXX

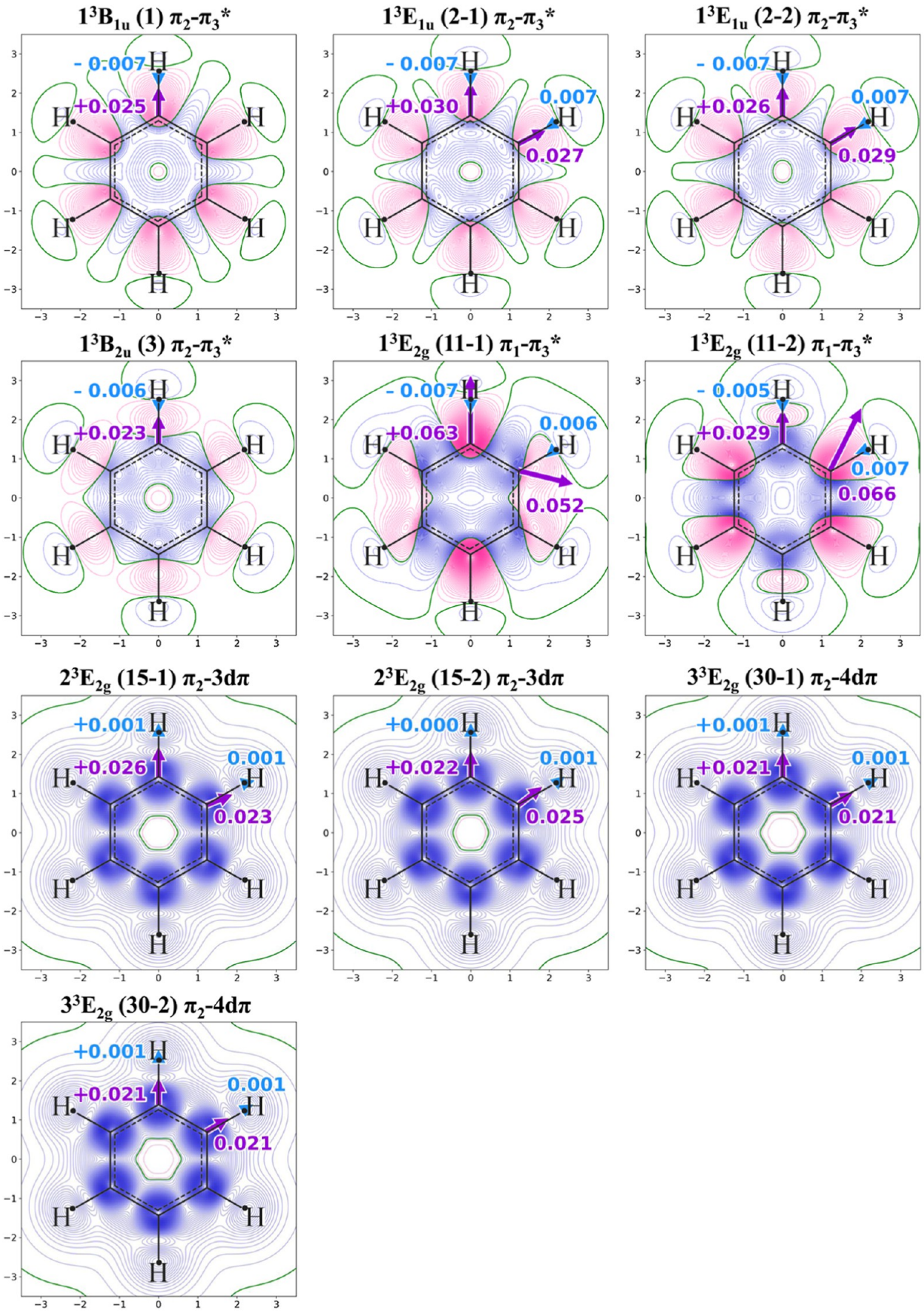

Figure 4. Force and density difference maps for Nos. 1, 2, 3, 11, 15, and 30 states of triplet excited states of benzene given in Table 1. Maps are on the plane 1 au above the benzene plane.

https://doi.org/10.1021/acs.jctc.5c02112
J. Chem. Theory Comput. XXXX, XXX, XXX−XXX

and the H−C bond will be shortened in all of these three valence triplet excited states.

As seen from Table 1, from Nos. 4 to 16, most states are from π_2 to 3s, 3p, and 3d Rydberg transitions, except for No. 11 state, which is the valence $\pi_1-\pi_3^*$ $^3E_{2g}$ state discussed later. These Rydberg states have second moments from 126−241 au. Excitation energies calculated by the present theory agree well with experiments, supporting the reliability of the present theory. Referring to Table 3, we see that forces acting on the C nucleus are about +0.011 ∼ + 0.026 au. The benzene ring will be enlarged in all of the Rydberg states. Referring to Figure S2 or those of Figure 3 with the same symmetry designations, density difference maps for these Rydberg states are similar because the Rydberg orbitals are much outside of the benzene ring, and what is written in these maps is only for the region close to the benzene ring, which should be similar for these states.

The No. 11 triplet state $^3E_{2g}$ mentioned above is special and very interesting. It is the triplet counterpart of the $^1E_{2g}$ state, discussed in some detail in the singlet section. For the triplet case, this state is the pure valence excited $\pi_1-\pi_3^*$ state, as seen from its second moment of only 89.6 au, though this value is slightly larger than that of the ground state, 78.4 au and the values for lower excited states, 79.0−80.8 au. This shows a small mixing of the Rydberg state. The present calculated excitation energy 7.596 eV is close to and within its literature value 7.49 ± 0.25 eV estimated by Lorentzon et al.[62] From Table 3, the force acting on carbon is remarkably large, 0.063−0.066 au, and therefore, the benzene ring will be enlarged in this excited state. On the other hand, the force acting on a proton is minus inward, like in the first three valence states $^3B_{1u}$, $^3E_{1u}$, and $^3B_{2u}$, and so the C−H bond would be shortened in this excited state. We note that its singlet counterpart, the $^1E_{2g}$ state, was not a valence state but mainly a Rydberg π_2-3dπ state, as discussed in the singlet section. As shown in Figure 4, the density difference map of this $^3E_{2g}$ state is a typical valence type, a transition from a valence bonding C−C region to valence antibonding C−C regions. Because two maps of degenerate states are slightly different, a small Jahn−Teller distortion may occur in this excited state.

Nos. 17 to 30 triplet states shown in Table 1 are mostly Rydberg excited states produced by excitations from the π_2 orbital to Rydberg 4s, 4p, and 4d orbitals. Among them, three pure valence $\sigma_8-\pi_3^*$excitations (Nos. 18−20) exist. We first discuss the Rydberg excited states. Though we do not know the experimental excitation energies, the calculated values are from 7.6 to 8.5 eV and are close to the experimental values estimated from singlet excitations. The calculated second moments are large from 417 to 487 au because they are excited Rydberg 4s, 4p, and 4d states. As seen from Table 3, forces acting on C nuclei are around 0.02 au, which work to expand the benzene ring. The forces acting on protons also elongate the C−H distance. In Figure 4, density difference maps of 2^3E_{2g} (No. 15) and 3^3E_{2g} (No. 30) states are shown. Their maps are both pure Rydberg type and similar to each other because the only difference is the Rydberg 3dπ and 4dπ orbitals that are outside of the maps. We showed these maps here because it is important to confirm that these two states are Rydberg in nature.

Three states, 2^3A_{2u}, 2^3E_{2u}, and 2^3A_{1u} (No. 18−20), are valence states due to $\sigma_8-\pi_3^*$ transitions, and their second moments are 79.8, 78.9, and 78.3 au, which are smaller than that of the triplet $^3E_{2g}$ state, 89.6 au. Forces acting on C and H nuclei shown in Table 3 are both to elongate the bond distances, but their magnitudes were small, predicting that the geometrical changes of these excited states should be very small. We note that density difference maps for these valence excited states were very similar to those of the corresponding singlet states shown in Figure 3. Therefore, geometrical changes induced for these triplet states should be similar to those already discussed previously for singlet states.

Thus, the present FC or SSE(SAC−CI, ESF) theory gave the results that reproduce well experimental data for triplet excited states. Valence−Rydberg mixing was found to be smaller in triplet excited states than in singlet excited states. This made the nature of the triplet excited states simpler than that of the singlet excited states. Among them, the second $^3E_{1u}$ $\pi_2-\pi_3^*$ excited state at 4.816 eV and the 11th $^3E_{2g}$ $\pi_1-\pi_3^*$ excited state at 7.596 eV were of special importance theoretically for their large differences from those in singlet excited states. The energy levels of these valence states in triplet states in contrast to those in singlet states relative to the Rydberg 3s, 3p, and 3d states were the key to big differences between singlet and triplet excited states of benzene.

4.3. Comparative Discussions between Singlet and Triplet Excited States of Benzene

After discussions on each of the singlet and triplet states are finished, it is interesting to compare these two groups of excited states. As is clear now, triplet excited states are much simpler than singlet states. Let us consider why? First, energetically, between two pairs of excitations from occupied orbital i to unoccupied orbital a, triplet excited states are more stable than singlet ones by twice the exchange integrals, $2K_{ia}$, which is positive. When both MO's i and a are valence, this exchange integral is large, and therefore, triplet excited states are largely more stable than the corresponding singlet ones. However, when a is Rydberg, the exchange integral becomes essentially zero, and so the singlet−triplet separation becomes very small. These trends are seen clearly in Table 1. The first three triplet states, $^3B_{1u}$, $^3E_{1u}$, and $^3B_{2u}$ (No. 1−3) are all $\pi_2-\pi_3^*$ excited states that are genuine valence states from doubly degenerate π_2 MO's to doubly degenerate π_3^* MO's. Therefore, their energies, 3.86−5.69 eV of the triplet, are much lower than 5.08−6.41 ∼ 7.09 eV of the singlet. On the other hand, for π_2-3s, 3pσ Rydberg excitations, Nos. 4, 5, and 6 triplet excitation energies, 6.37, 6.88, and 7.00 eV are close to those of singlet, 6.42, 6.95, and 7.02 eV. Similarly, for π_2-4s, 4pσ Rydberg excitations, Nos. 17, 18, and 19 triplet excitation energies, 7.96, 8.12, and 8.16 eV are close to those of singlet cases, 7.97, 8.14, and 8.16 eV, being closer than π_2-3s, 3pσ Rydberg cases as expected.

With this knowledge in mind, we want to study more about the natures of E_{1u} and E_{2g} states of benzene. For valence states, E_{1u} is related to $\pi_2-\pi_3^*$ excitations, and E_{2g} is to $\pi_1-\pi_3^*$ excitations: they are two key states among many excited states of this molecule, and their differences between singlet and triplet states seem to show important physics. First, let us consider the E_{1u} states. In triplets, whose energy is lower than singlets by $2K_{ia}$ for valence states, the lowest three valence $\pi_2-\pi_3^*$ excited states, $^3B_{1u}$, $^3E_{1u}$, and $^3B_{2u}$ are far below 6.37 eV, which is the first Rydberg state, π_2-3s $^3E_{1g}$ state. Therefore, valence-Rydberg mixing cannot occur. This is one origin of the simpleness of the triplet excited state. The first three (or four, including degeneracy) valence states could be free from the mixing of Rydberg states. Then, separately above the valence $\pi_2-\pi_3^*$ $^3B_{2u}$ excitation, the π_2-Rydberg 3s, 3p, 3d excitations continue until the No. 10 $^3B_{2g}$ state. Then, the $\pi_1-\pi_3^*$ $^3E_{2g}$ transition is calculated at 7.596 eV, which is close to and within its literature

https://doi.org/10.1021/acs.jctc.5c02112
J. Chem. Theory Comput. XXXX, XXX, XXX−XXX

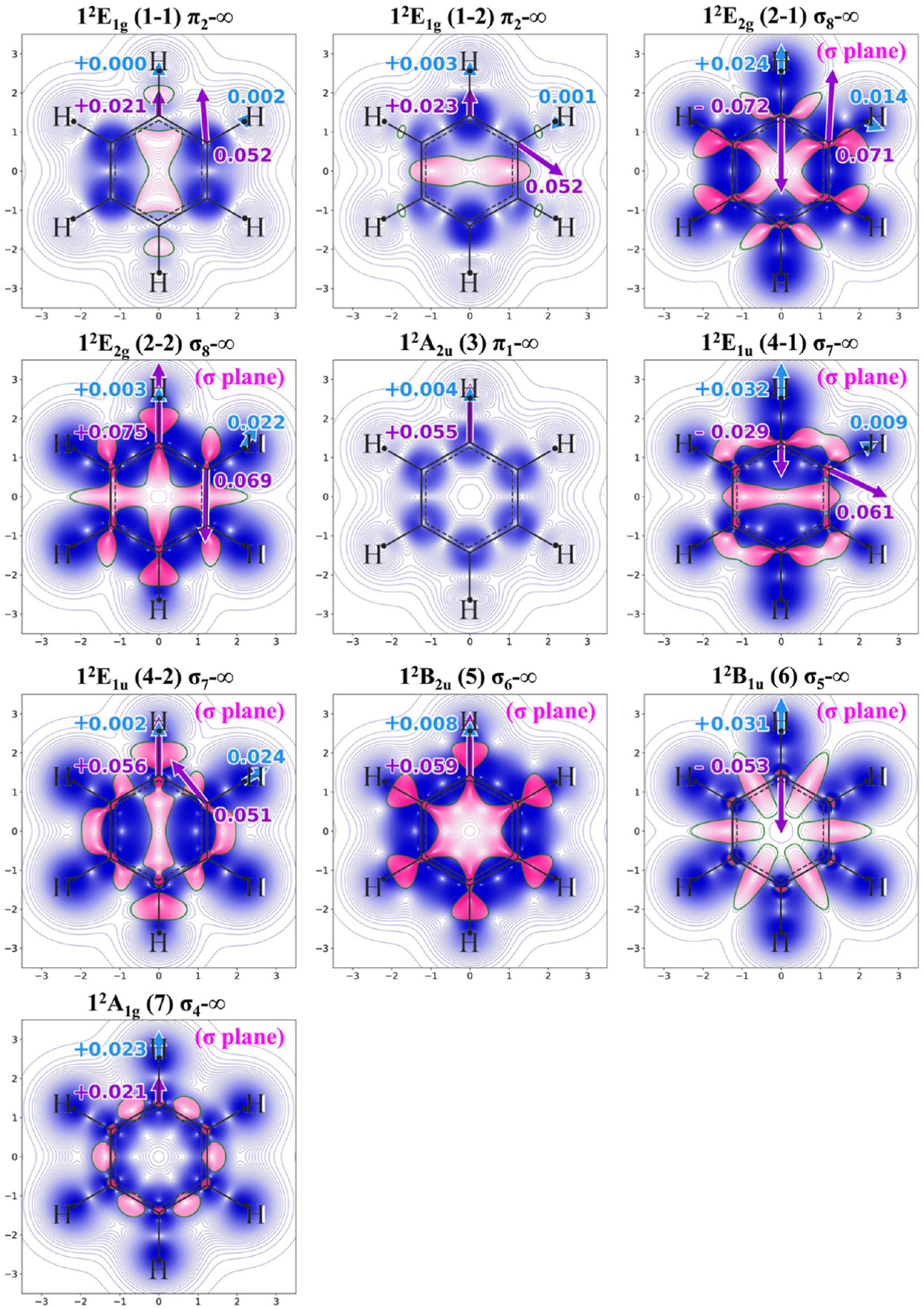

Figure 5. Force and density difference maps for ionized states of benzene given in Table 1. Green, red, and blue lines mean zero, plus, and minus, respectively. The map on the molecular plane is given marked as theσ plane and the other map without a mark is on the plane 1 au above the benzene plane.

https://doi.org/10.1021/acs.jctc.5c02112
J. Chem. Theory Comput. XXXX, XXX, XXX−XXX

value of 7.49 ± 0.25 eV estimated by Lorentzon et al.[62] This state is almost pure valence, as seen clearly from the second moment value, 89.6 au of Table 1, and also from its difference density map shown in Figure 4. This energy, 7.596 eV, is lower than the comparable 7.822 eV of the singlet case. The author does not yet clearly understand why this $\pi_1-\pi_3^*$ 1^3E_{2g} state was free from valence-Rydberg mixing. One possibility is the difference of the excitation space between π and σ. Namely, below and above this $\pi_1-\pi_3^*$ 1^3E_{2g} state, there are two π_2-3dσ states with separations of 0.464 and 0.146 eV, respectively, from the next π_2-3dπ states, 2^3E_{1u} No. 8, and 1^3A_{1g} No. 14 states. Though in triplet, this No. 11 1^3E_{2g} state was a pure valence state, two higher $^3E_{2g}$ states at No. 15 and No. 30 states were both pure Rydberg $\pi_2 \rightarrow 3d\pi$ and $\pi_2 \rightarrow 4d\pi$ states, respectively, as seen from Table 1 and from their density difference maps shown in Figure 4.

4.4. Ionized States

For one-electron ionized states, the Koopmans model based on the molecular orbital model is a first approximation of their electronic states. In Table 1, next to state designations, we gave theoretical values of ionization energies of benzene calculated with the present theory compared with experimental values, differences, Δ(IE) = theory − experiment, peak intensities in ionization spectra calculated by the monopole approximation, and second moments of ionized states. To see the change of the electron density in the π or σ region, depending on the nature of the ionization, we gave in Figure 5 the density difference map for either the π or σ region caused by the ionization. The outermost line shows the zero-density line. Thereby, induced forces acting on carbon and hydrogen nuclei are also given.

The ordering of ionization energies (IEs) follows that of the occupied molecular orbital energies. The IEs calculated with the present theory agreed with experimental values to within 0.24 eV, except for the $^2E_{2g}(\sigma_8 \rightarrow \infty)$ state, which was previously noted as "approximate".[64] All ionized states have similar second moments close to the average value, 57.5 au, which is much smaller than that of the ground state, 78.4 au. Because ionized states have one excess positive charge on the nuclear framework, it pulls all electron clouds toward the nuclear framework, and so ionized states become slim, and second moments become smaller than those of the neutral state. The intensity of the ionization peak of each state is also close to the average value, 0.889.

The nature of each ionized state is understood from the density difference map and induced forces shown in Figure 5. The first ionized state is from the degenerate π_2 orbitals, and density differences and induced forces are shown as 1^2E_{1g} (1−1) and (1−2) $\pi_{2-\infty}$. Two maps of degenerate ionizations seem to suggest different geometrical changes, and thus, this degenerate ionization seems to cause a Jahn−Teller distortion. The second ionized state, 1^2E_{2g} (2−1) and (2−2) $\sigma_{8-\infty}$, is from the degenerate σ_8 orbital. Again, as seen from the interesting set of maps, this degenerate ionization seems to cause a Jahn−Teller distortion. Actual follow-ups of these Jahn−Teller distortions are interesting. The next ionized state, 1^2A_{2u} (No. 3) is the nondegenerate ionization from the lowest π_1 bonding orbital. It causes an elongation of the C−C bond. The next degenerate 1^2E_{1u} (No. 4) ionization is as large as 14.347 eV. It is the ionization from the degenerate σ_7 orbital and would cause Jahn−Teller distortion of the C−C and C−H bonds. Thus, all degenerate ionizations of benzene seem to cause Jahn−Teller distortions. The next three ionizations (Nos. 5, 6, and 7) are all from σ-type deep orbitals, and their ionization energies were 14.780, 15.761, and 17.284 eV. From their difference density maps, these three ionizations are roughly from C−C, C−H, and all regions, respectively. These high-energy ionizations must cause big changes in the bonding and, therefore, big structural changes of the benzene molecule. The maps presented here show only the initial stage. Further detailed examinations are very interesting.

5. CONCLUDING REMARKS

In this paper, a new highly accurate and general quantum chemical theory, called the FC(SAC−CI, ESF) or SSE(SAC−CI, ESF) theory, has been developed for studying ground, excited, and ionized states of molecules using energy and force concepts. The FC or SSE theory for solving the scaled Schrödinger equation[4−6] is an exact theory that can elevate not only molecular wave functions but also their theories themselves from some initial levels to the truly exact level. Here, this theory has been applied, within the level of integral theories not including g_{ij}-functions, to the SAC−CI theory for molecular ground and excited states,[16−20,26−31] using basis sets that satisfy the Hellmann−Feynman electrostatic force theorem,[36−39] which guarantees the use of pictorial and intuitive force concepts developed by this author.[39−46] With this FC(SAC−CI, ESF) formalism, the SAC/SAC−CI method[16,17] that satisfies the Hellmann−Feynman theorem has been elevated to a highly accurate level, as seen from the last diagram of Figure 1 obtained by applications to the benzene molecule. This enables the use of not only energetic concepts but also intuitive ESF concepts together with dynamic electron density concepts for molecular geometries and chemical reactions.[40−45] This theory was used to study what happens to benzene's structure after excitations and ionizations. Nondegenerate Ag, Au, Bg, and Bu states may keep their high symmetry, but degenerate Eg and Eu states may even break their structure of high symmetry toward lower symmetries. Density difference maps and force vectors acting on nuclei in degenerate states could predict such possible structural changes.

The energy concept is useful to understand the energy levels and stabilities of various excited and ionized states, and the force and density concepts are useful for predicting the direction of the geometrical change in each vertical excited and ionized state. Indeed, induced forces and density difference maps we used in this paper for predicting geometrical changes that occur at vertical excited and ionized states are not the energy concept but the force concept. Energy is only a single scalar quantity, but density reorganization caused by excitation and ionization is pictorial three-dimensional information, and the force acting on each nucleus of the system is a three-dimensional vector that leads to predictions of phenomena that occur after excitations and ionizations. The present theory is designed to be able to use both energies and forces, two basic quantities, for studying many different chemistries of singlet and triplet excited states and ionized states. Here, this theory has been applied to a benzene molecule.

Among 28 lower singlet vertical excited states below 8.5 eV studied here, only the first two $\pi_2-\pi_3^*$ transitions and another three $\sigma_8-\pi_3^*$ transitions at 8.21−8.28 eV, altogether five states, were valence states. Other states were mixed valence-Rydberg or pure Rydberg states. Among 30 lower triplet vertical excited states below 8.5 eV, the first three $\pi_2-\pi_3^*$ states, 1^3E_{2g} (No. 11) $\pi_1-\pi_3^*$ at 7.596 eV, and three $\sigma_8-\pi_3^*$ excited states at 8.00−8.04 eV, altogether seven states were valence states. Altogether,

https://doi.org/10.1021/acs.jctc.5c02112
J. Chem. Theory Comput. XXXX, XXX, XXX−XXX

among 58 lower excited states below 8.5 eV of benzene, 12 states were valence states, and other states were Rydberg-mixed or pure Rydberg states. It is interesting to study higher excited states, particularly the valence-nature singlet $\pi_1-\pi_3^*$ excited state of $^1E_{2g}$ symmetry, because experimentally Yoshihara et al. reported it to be at 9.4 eV in solution.[61] In the present study, we included Rydberg orbitals of only up to 4s, 4p, and 4d states, which limited the present study to be below 8.5 eV. We plan to study higher than 8.5 eV excited states of benzene in the near future.

Important similarities and differences were found between the singlet and triplet states of benzene. For valence states, excitation energies were much different between singlets and triplets of the same space symmetry, though the density difference maps were similar. For Rydberg states, on the other hand, both excitation energies and density difference maps were similar in the molecular region when their symmetries were the same. A key to this large difference lies in the difference in exchange repulsion integrals between valence and Rydberg excitations: these integrals are large for valence excitations but negligibly small for Rydberg excitations. Due to this and many other important factors, the total stories of excited and ionized states of the benzene molecule were described here highly accurately by the scaled Schrödinger equation theory or the FC theory combined with the SAC/SAC−CI and ESF theories.

■ ASSOCIATED CONTENT

Supporting Information

The Supporting Information is available free of charge at https://pubs.acs.org/doi/10.1021/acs.jctc.5c02112.

Force and difference density maps for all excited states of a benzene molecule studied in this paper for singlet and triplet excited states (PDF)

■ AUTHOR INFORMATION

Corresponding Author

Hiroshi Nakatsuji − *Kyoto Technoscience Center 16, Quantum Chemistry Research Institute, Sakyo-ku, Kyoto 606-8305, Japan;* orcid.org/0000-0002-8162-3220; Email: h.nakatsuji@qcri.or.jp

Complete contact information is available at: https://pubs.acs.org/10.1021/acs.jctc.5c02112

Notes

The author declares no competing financial interest.

■ ACKNOWLEDGMENTS

The author acknowledges Dr. Hiroyuki Nakashima for his kind assistance in computations and discussions and Dr. Yusaku I. Kurokawa for collaborations. He also acknowledges the computer center of the Research Center for Computational Science in the Institute of Molecular Science (IMS), Okazaki, Japan, for huge support and encouragements given to us. In particular, we would like to appreciate Prof. M. Ehara and K. Suzuki for their generous and technical support in using their superparallel machines efficiently. This work was supported by JSPS KAKENHI grant numbers 22H02045 and 23K23313.

■ REFERENCES

(1) Kaku, M. *The God Equation: The Quest for a Theory of Everything*; Stuart Krichevsky Literary Agency, Inc.: New York, 2021.

(2) Dirac, P. A. M. The quantum theory of the electron. *Proc. R. Soc. A* **1928**, *117*, 610−624.

(3) Nakatsuji, H. Structure of the exact wave function. *J. Chem. Phys.* **2000**, *113*, 2949−2956.

(4) Nakatsuji, H. Scaled Schrödinger equation and the exact wave function. *Phys. Rev. Lett.* **2004**, *93*, 030403.

(5) Nakatsuji, H. General method of solving the Schrödinger equation of atoms and molecules. *Phys. Rev. A:At., Mol., Opt. Phys.* **2005**, *72*, 062110.

(6) Nakatsuji, H. Discovery of a general method of solving the Schrödinger and Dirac equations that opens a way to accurately predictive quantum chemistry. *Acc. Chem. Res.* **2012**, *45*, 1480−1490.

(7) Kurokawa, Y.; Nakashima, H.; Nakatsuji, H. Free ICI (Iterative Complement Interaction) Calculations of Hydrogen Molecule. *Phys. Rev. A:At., Mol., Opt. Phys.* **2005**, *72*, 062502.

(8) Nakashima, H.; Nakatsuji, H. Solving the Schrödinger equation for helium atom and its isoelectronic ions with the free iterative complement interaction (ICI) method. *J. Chem. Phys.* **2007**, *127*, 224104.

(9) Kurokawa, Y.; Nakashima, H.; Nakatsuji, H. Solving the Schrödinger equation of helium and its isoelectronic ions with the exponential integral (Ei) function in the free iterative complement interaction method. *Phys. Chem. Chem. Phys.* **2008**, *10*, 4486−4494.

(10) Nakatsuji, H.; Nakashima, H. Solving the Schrödinger equation of molecules by relaxing the anti-symmetry rule: Inter-exchange theory. *J. Chem. Phys.* **2015**, *142*, 194101.

(11) Nakatsuji, H.; Nakashima, H.; Kurokawa, Y. I. Solving the Schrödinger equation of atoms and molecules: Chemical-formula theory, free-complement chemical-formula theory, and intermediate variational theory. *J. Chem. Phys.* **2018**, *149*, 114105.

(12) Nakatsuji, H.; Nakashima, H.; Kurokawa, Y. I. Solving the Schrödinger equation of atoms and molecules with the free-complement chemical-formula theory: First-row atoms and small molecules. *J. Chem. Phys.* **2018**, *149*, 114106.

(13) Nakatsuji, H.; Nakashima, H. Potential curves of the lower nine states of Li_2 molecule: Accurate calculations with the free complement theory and the comparisons with the SAC/SAC-CI results. *J. Chem. Phys.* **2022**, *157*, 094109.

(14) Nakatsuji, H.; Nakashima, H.; Kurokawa, Y. I. Accurate scaling functions of the scaled Schrödinger equation. *J. Chem. Phys.* **2022**, *156*, 014113.

(15) Nakatsuji, H.; Nakashima, H. Accurate scaling functions of the scaled Schrödinger equation. II.Variational examination of the correct scaling functions with the free complement theory applied to the helium atom. *J. Chem. Theory Comput.* **2024**, *20*, 3749−3765.

(16) Nakatsuji, H.; Hirao, K. Cluster expansion of the wavefunction. Symmetry-adapted-cluster expansion, its variational determination, and extension of open-shell orbital theory. *J. Chem. Phys.* **1978**, *68*, 2053−2065.

(17) Nakatsuji, H. Cluster Expansion of the Wavefunction. Excited States. *Chem. Phys. Lett.* **1978**, *59*, 362−364.

(18) Nakatsuji, H. Exponentially generated wave functions. *J. Chem. Phys.* **1985**, *83*, 5743−5748.

(19) Nakatsuji, H. Electronic-structures of ground, excited, ionized, and anion states studied by the SAC/SAC-CI theory. *Acta Chim. Hung. Model. Chem.* **1992**, *129*, 719−776.

(20) Nakatsuji, H. SAC-CI method: Theoretical aspects and some recent topics. In *Computational chemistry - Reviews of current trends*; Leszczynski, J., Ed.; World Scientific, 1997; Vol. 2, pp 62−124..

(21) Coester, F. Bound states of a many-particle system. *Nucl. Phys.* **1958**, *7*, 421−424.

(22) Coester, F.; Kümmel, H. Short-range correlations in nuclear wave functions. *Nucl. Phys.* **1960**, *17*, 477−485.

(23) Sinanoğlu, O. Many-electron theory of atoms and molecules. I. Shells, electron pairs vs many-electron correlations. *J. Chem. Phys.* **1962**, *36*, 706−717.

(24) Cizek, J. On the Correlation Problem in Atomic and Molecular Systems. Calculation of Wavefunction Components in Ursell-Type

Expansion Using Quantum-Field Theoretical Methods. *J. Chem. Phys.* **1966**, *45*, 4256−4266.
(25) Cizek, J.; Paldus, J.; Sroubkova, L. Cluster Expansion Analysis for Delocalized Systems. *Int. J. Quantum Chem.* **1969**, *3*, 149−167.
(26) Kitao, O.; Nakatsuji, H. Cluster Expansion of the Wavefunction. Valence and Rydberg Excitations and Ionizations of Benzene. *J. Chem. Phys.* **1987**, *87*, 1169−1182.
(27) Nakatsuji, H.; Ehara, M. Collision Induced Absorption Spectra of CeXe System Studied by the SAC-CI Theory. *Chem. Phys. Lett.* **1990**, *172*, 261−264.
(28) Ehara, M.; Ohtsuka, Y.; Nakatsuji, H.; Takahashi, M.; Udagawa, Y. Theoretical Fine Spectroscopy with SAC-CI Method: Outer- and Inner-Valence Ionization Spectra of Furan, Pyrrole, and Thiophene. *J. Chem. Phys.* **2005**, *122*, 234319.
(29) Nakatsuji, H.; Hasegawa, J.; Ohkawa, K. Rhodopseudomonas viridis, Excited States and Electron Transfer Mechanism in the Photosynthetic Reaction Cente of *Rhodopseudomonas Viridis*: SAC-CI Study. *Chem. Phys. Lett.* **1998**, *296*, 499−504.
(30) Ito, H.; Nakatsuji, H. The Role of Proteins in the Electron Transfer in the Photosynthetic Reaction Center of *Rhodopseudomonas Viridis*: Bacteriopheophytin to Ubiquinone. *J. Comput. Chem.* **2001**, *22*, 265−272.
(31) Nakatani, N.; Hasegawa, J.; Nakatsuji, H. Artificial color tuning of firefly luminescence: Theoretical mutation by tuning electrostatic interactions between protein and luciferin. *Chem. Phys. Lett.* **2009**, *469*, 191−194.
(32) Frisch, M. J.; Trucks, G. W.; Schlegel, H. B.; Scuseria, G. E.; Robb, M. A.; Cheeseman, J. R.; Scalmani, G.; Barone, V.; Petersson, G. A.; Nakatsuji, H.; Li, X.; Caricato, M.; Marenich, A. V.; Bloino, J.; Janesko, B. G.; Gomperts, R.; Mennucci, B.; Hratchian, H. P.; Ortiz, J. V.; Izmaylov, A. F.; Sonnenberg, J. L.; Williams-Young, D.; Ding, F.; Lipparini, F.; Egidi, F.; Goings, J.; Peng, B.; Petrone, A.; Henderson, T.; Ranasinghe, D.; Zakrzewski, V. G.; Gao, J.; Rega, N.; Zheng, G.; Liang, W.; Hada, M.; Ehara, M.; Toyota, K.; Fukuda, R.; Hasegawa, J.; Ishida-Endo, M.; Nakajima, T.; Honda, Y.; Kitao, O.; Nakai, H.; Vreven, T.; Throssell, K.; Montgomery, J. A., Jr.; Peralta, J. E.; Ogliaro, F.; Bearpark, M. J.; Heyd, J. J.; Brothers, E. N.; Kudin, K. N.; Staroverov, V. N.; Keith, T. A.; Kobayashi, R.; Normand, J.; Raghavachari, K.; Rendell, A. P.; Burant, J. C.; Iyengar, S. S.; Tomasi, J.; Cossi, M.; Millam, J. M.; Klene, M.; Adamo, C.; Cammi, R.; Ochterski, J. W.; Martin, R. L.; Morokuma, K.; Farkas, O.; Foresman, J. B.; Fox, D. J. *Gaussian Software Package, GAUSSIAN 16*. Revision GDV J. 28; Gaussian, Inc: Wallingford CT, 2024.
(33) Geertsen, J.; Rittby, M.; Bartlett, R. J. The equation-of-motion coupled-cluster method: Excitation energies of Be and CO. *Chem. Phys. Lett.* **1989**, *164*, 57−62.
(34) Stanton, J. F.; Bartlett, R. J. The equation of motion coupled-cluster method. A systematic biorthogonal approach to molecular excitation energies, transition probabilities, and excited state properties. *J. Chem. Phys.* **1993**, *98*, 7029−7039.
(35) SAC-CI GUIDE. *Welcome to SAC-CI Home Page on*; Nakatsuji Laboratory 2012; pp 30−32 https://qcri.or.jp/sacci.
(36) Hellmann, H. *Einfuhrung in Die Quantenchemie*; Deuticke: Leipzig, 1937.
(37) Feynman, R. P. Forces in Molecules. *Phys. Rev.* **1939**, *56*, 340−343.
(38) Hurley, A. C. *Introduction to the Electron Theory of Small Molecules*; Academic Press Inc.: London, 1976.
(39) Nakatsuji, H.; Kanda, K.; Yonezawa, T. Force in SCF Theories. *Chem. Phys. Lett.* **1980**, *75*, 340−346.
(40) Nakatsuji, H. Electrostatic force theory for a molecule and interacting molecules I. Concept and illustrative applications. *J. Am. Chem. Soc.* **1973**, *95*, 345−354.
(41) Nakatsuji, H. Electrostatic force theory for a molecule and interacting molecules II. Shapes of the ground- and excited-state molecules. *J. Am. Chem. Soc.* **1973**, *95*, 354−361.
(42) Nakatsuji, H. Common Natures of the Electron Cloud of the System Undergoing Change in Nuclear Configuration. *J. Am. Chem. Soc.* **1974**, *96*, 24−30.
(43) Nakatsuji, H. Electron-cloud following and preceding and the shapes of molecules. *J. Am. Chem. Soc.* **1974**, *96*, 30−37.
(44) Deb, B. M. *The Force Concept in Chemistry*; Van Nostrand Reinhold Co.: New York, 1981.
(45) Nakatsuji, H.; Koga, T. *Force Models for Molecular Geometry. in Deb's Book (Ref. 44)*.
(46) Bader, R. F. W. *The Nature of Chemical Binding. in Deb's Book (Ref. 44)*.
(47) Herzberg, G. *Electronic Spectra and Electronic Structure of Polyatomic Molecules*; Van Nostrand: New York, 1966.
(48) Slater, J. C. Atomic shielding constants. *Phys. Rev.* **1930**, *36*, 57−64.
(49) Dunning, Jr., T. H.; Hay, P. J. *Methods of Electronic Structure Theory*, Schaefer, H. F., III, Ed.; Plenum Press: New York, 1977; pp 1−28.
(50) Estimated from the experimental atomization energy and the zero-point vibrational energy, given by NIST chemistry webbook (see https://webbook.nist.gov/chemistry/) and ref 12.
(51) Eriksen, J. J.; Anderson, T. A.; Deustua, J. E.; Ghanem, K.; Hait, D.; Hoffmann, M. R.; Lee, S.; Levine, D. S.; Magoulas, I.; Shen, J.; Tubman, N. M.; Whaley, K. B.; Xu, E.; Yao, Y.; Zhang, N.; Alavi, A.; Chan, G. K.-L.; Head-Gordon, M.; Liu, W.; Piecuch, P.; Sharma, S.; Ten-no, S. L. U.; Umrigar, C. J.; Gauss, J. The Ground State Electronic Energy of Benzene. *J. Phys. Chem. Lett.* **2020**, *11*, 8922−8929.
(52) Lassettre, E. N.; Skerbele, A.; Dillon, M. A.; Ross, K. J. High-Resolution Study of Electron-Impact Spectra at Kinetic Energies between 33 and 100 eV and Scattering Angles to 16°. *J. Chem. Phys.* **1968**, *48*, 5066−5096.
(53) Johnson, P. M. The multiphoton ionization spectrum of benzene. *J. Chem. Phys.* **1976**, *64*, 4143−4148.
(54) Johnson, P. M.; Koronowski, G. M. The discovery of a 3p rydberg state in benzene by three-photon resonant multiphoton ionization spectroscopy. *Chem. Phys. Lett.* **1983**, *97*, 53−56.
(55) Wilkinson, P. G. Absorption Spectra of Benzene and BENZENE-d_6 in the Vacuum Ultraviolet. *Can. J. Phys.* **1956**, *34*, 596−615.
(56) Dawes, A.; Pascual, N.; Hoffmann, S. V.; Jones, N. C.; Mason, N. J. Vacuum ultraviolet photoabsorption spectroscopy of crystalline and amorphous benzene. *Phys. Chem. Chem. Phys.* **2017**, *19*, 27544−27555.
(57) Whetten, R. L.; Grubb, S. R.; Otis, C. E.; Albrecht, A. C.; Grant, E. R. Higher excited states of benzene: Polarized ultraviolet two-photon absorption spectroscopy. *J. Chem. Phys.* **1985**, *82*, 1115−1134.
(58) Grubb, S. R.; Otis, C. E.; Whetten, R. L.; Grant, E. R.; Albrecht, A. C. Higher excited states of benzene: Symmetry assignments of six gerade Rydberg series by four-photon absorption spectroscopy. *J. Chem. Phys.* **1985**, *82*, 1135−1146.
(59) Nakashima, N.; Sumitani, M.; Ohmine, I.; Yoshihara, K. Nanosecond laser photolysis of the benzene monomer and eximer. *J. Chem. Phys.* **1980**, *72*, 2226−2230.
(60) Nakashima, N.; Inoue, H.; Sumitani, M.; Yoshihara, K. Yoshihara, Laser flash photolysis of benzene. II. Laser-induced cluster formation in gas phase. *J. Chem. Phys.* **1980**, *73*, 4693−4694.
(61) Nakashima, N.; Inoue, H.; Sumitani, M.; Yoshihara, K. Yoshihara, Laser flash photolysis of benzene. III. $S_n \leftarrow S_1$ absorption of gaseous benzene. *J. Chem. Phys.* **1980**, *73*, 5976−5980.
(62) Lorentzon, J.; Malmqvist, P.; Fülscher, M.; Roos, B. O. A CASPT2 study of the valence and lowest Rydberg electronic states of benzene and phenol. *Theor. Chim. Acta* **1995**, *91*, 91−108.
(63) Doering, J. P. Low-energy electron-impact study of the first, second, and third triplet states of benzene. *J. Chem. Phys.* **1969**, *51*, 2866−2870.
(64) Baltzer, P.; Karlsson, L.; Wannberg, B.; Öhrwall, G.; Holland, D. M. P.; MacDonald, M. A.; Hayes, M. A.; von Niessen, W. An experimental and theoretical study of the valence shell photoelectron spectrum of the benzene molecule. *Chem. Phys.* **1997**, *224*, 95−119.

https://doi.org/10.1021/acs.jctc.5c02112
J. Chem. Theory Comput. XXXX, XXX, XXX−XXX